IDENTIFICATION AND CONTROL OF WHITE WATER RECYCLE SYSTEMS

By

Huiping Chen

B. A. Sc. Shanghai Jiao Tong University

A THESIS SUBMITTED IN PARTIAL FULFILLMENT OF

THE REQUIREMENTS FOR THE DEGREE OF

MASTER OF APPLIED SCIENCE

in

THE FACULTY OF GRADUATE STUDIES

DEPARTMENT OF ELECTRICAL AND COMPUTER ENGINEERING

We accept this thesis as conforming

to the required standard

THE UNIVERSITY OF BRITISH COLUMBIA

February 1998

In presenting this thesis in partial fulfilment of the requirements for an advanced degree at the University of British Columbia, I agree that the Library shall make it freely available for reference and study. I further agree that permission for extensive copying of this thesis for scholarly purposes may be granted by the head of my department or by his or her representatives. It is understood that copying or publication of this thesis for financial gain shall not be allowed without my written permission.

Department of Electrical and Computer Enginnering
The University of British Columbia
2075 Wesbrook Place
Vancouver, Canada
V6T 1Z1

Date: Feb. 23, 1998

Abstract

In recent years, more environmental restrictions have been imposed on pollutant discharge and fresh water consumption from paper mills. This gives increasing motivation to industry for closing paper machine white water system. With inter-related recycle loops, the white water system exhibits complicated dynamics. Identification and control of such a system in the presence of dynamics uncertainty is the primary goal of this research. Motivated by its simplicity and strong features in modelling unstructured processes, the Laguerre series representation is chosen for system modelling and on-line identification. A controller for the white water recycle system must be able to handle unmeasurable disturbances, process time delays, interactions inside and outside the plant etc. It has been proved that generalized predictive control (GPC) is a robust algorithm for adaptive applications. This research presents the first application of the Laguerre model based adaptive GPC for the control of the recycle system. Simulation results show that this control scheme provides excellent servo performance and load disturbance rejection.

Table of Contents

List of Figures

Acknowledgements

I would like to express my deep gratitude to my supervisors Dr. Guy Dumont and Dr. Ezra Kwok for their valuable guidance and kind support. I would also like to thank Dr. Michael Davies for his assistance and input during the process of this research.

I thank all my friends at UBC Pulp and Paper Centre for their help and valuable discussion, deserving special mention to Ping Li, Ming Zhang, Roger Shirt and Lahoucine Ettaleb.

I am most grateful to my husband, Kangming Liu, for his support and patience during the long process of this thesis.

Dedication

This thesis is dedicated to the memory of my parents.

Chapter 1

Introduction

This thesis is focused on paper machine white water recirculation dynamics. The subject is the on-line estimation and adaptive control of the white water recycle system based on Laguerre models. This chapter provides the background on paper machine white water systems and a description of the challenging problems of processes with recycle loops. It is concluded with an overview of the thesis.

1.1 Background

1.1.1 White Water System

In the wet end of a paper machine, water from the wet web is drained through the wire during web formation. This water contains various proportions of fibres, fillers, fines and some other chemicals. These substances can be re-used by recirculating the water-called *white water*- to previous stages of the process, so that water usage and product loss can be minimized. Therefore, the basic objectives in closing the paper mill white water system are to maximize white water reuse and minimize the discharge of pollutants in paper mill effluents. In other words, recycling white water can decrease fibre losses and fresh water demand in the system.

In the white water system (See Figure 1.1), the *thick stock* is diluted with the white water. Then the diluted stock (*thin stock*), at the consistency required at the headbox, is cleaned, deaerated and screened before it reaches the headbox. The stock is jetted out from the open slice of the headbox and distributed across the wire. To achieve a homogeneous distribution, there is an overflow channel, through which the overflow is recirculated to the bottom of the wire pit and goes to the fan pump. In the wire section, the sheet is formed between two wires.

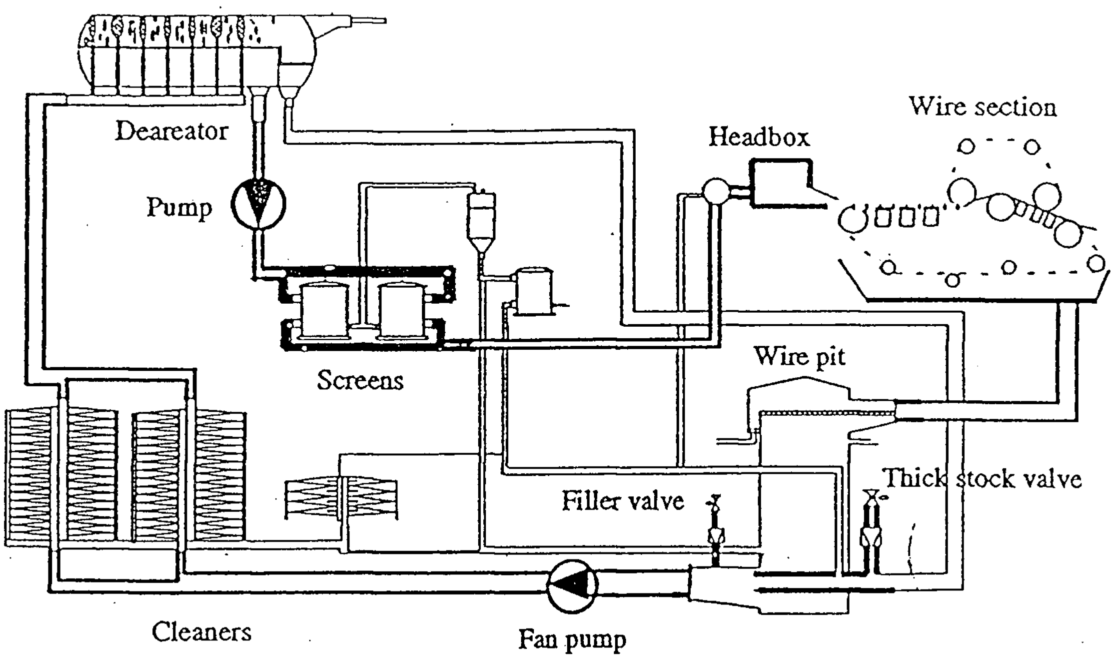

Figure 1.1: White water system [14]

Most of the water drains through the bottom wire, while a large percentage of fibre stays on and is carried by the wire to the press section. The white water, drained from the wire section, is collected in the wire pit. Again in the bottom of the wire pit, the white water is mixed with the thick stock to give the stock a suitable consistency. The white water is also used in the cleaners to dilute the rejects flow to a consistency suitable for subsequent cleaner inlets. The level in the wire pit is kept constant with an overflow channel.

The total amount of solids (fines, fillers, fibres and others) in the white water depends on the quality of paper produced and the equipment used. In this system, the wet web consistency can be controlled by the thick stock flowrate to regulate paper properties, but the white water recycle also affects paper machine performance, product quality and uniformity. The stability of operation in the paper machine depends on the paper machine performance efficiencies and the method of white water closure.

1.1.2 Literature Review of Recycle Systems

Systems that contain recycle streams are quite common in industry. Typically recycle dynamics are found in a process where an unreacted reactant or unused substance is separated from the product and fed back to the previous stage of the process for re-use. The dynamics and control of individual process units are well understood at present, but if recycle streams exist in the plant, the process can exhibit complicated dynamics. The procedure for control design becomes poorly understood. Only limited research has taken place in this area and only a few papers regarding recycle dynamics have been published in the past three decades.

One of the earliest papers by Gilliland et al.(1964) [1] considered a simplified reactor /distillation column process to study the characteristics of recycle systems. They were one of the first to point out that the recycle increases the overall time constant of a process, thus making control system performance more sluggish. Verykios and Luyben (1978) [2] explored some steady state and dynamic properties of a simple reactor /column system with recycle. The recycle flowrate varied considerably at a steady state for changes in feed conditions, and affected the dynamic characteristics of the plant. The higher recycle flowrate generally results in a more underdamped system.

Luyben and Buckley (1977) [3] discussed the liquid level control of a liquid recycle system in a plantwide environment. There are two conflicting objectives for the controller design. The major purpose of the level control is to keep the level at its desired operating condition. On the other hand, the outflow changes should be as smooth as possible in order to avoid disturbing downstream units. They proposed a combined proportional-only feedback control and feedforward control to achieve smooth flowrate changes without offset in liquid level.

Denn(1982) [4] showed some inherent properties of recycle systems. It was shown that a system with recycle has a larger time constant and a higher steady state gain than a process without recycle. This conclusion was later supported by the work of Kapoor and Marlin(1986) [5]. Denn also mentioned that the recycle makes a plant more sensitive to low frequency disturbances. This is a direct result of the time constant increase.

Luyben(1988) [6] developed a concept that he named "eigenstructure", which refers to the best control structure for rejecting load disturbances. He also found that every process has an intrinsically self-regulating control structure. So the first step for controller design is to find this structure for the particular control purpose.

In a series of papers about the dynamics and control of recycle systems, Luyben(1993)[7, 8, 9] more recently derived some important results for recycle systems based on a reactor/distillation column configuration with recycle. It was demonstrated that the behavior of a recycle system depends strongly on the recycle loop gain, and that the dynamics of the individual units in the recycle loop also affect the system performance. He explored the tradeoffs between steady state design and controllability by comparing different process designs. In a reactor/two distillation column system with recycle, changes in fresh feed flow rate have the most dramatic effect on the system. A small change in fresh feed can lead to a great increase in the flow rate of the recycle stream. Based on this result, he concluded a generic rule for recycle systems: The point in the control of recycle systems is to fix the flowrate somewhere in the recycle loop so that a "snowball" effect cannot occur.

A newly published paper[10] by Belanger and Luyben (1997) considered the effects of inventory control tuning on plantwide regulatory performance based on frequency domain analysis. They found that the amplification of the effects of load disturbances on controlled variables caused by material recycle was affected by two factors: the recycle gain and the tuning of the inventory controllers within the recycle loop. Bode plots revealed that the recycle gain affects the amplification at low frequencies, while the gains of the inventory controllers in the recycle loop affect the breakpoint frequencies of the recycling function.

Most of the above discussions are based on a reactor/distillation column configuration. But it is generally believed that these phenomena and dynamic properties are quite generic to almost any recycle system. So those generic guidelines and control design methodology can be used to guide the research concerning the processes with recycle streams. There are still a lot of unanswered questions associated with the dynamics and control of recycle systems.

1.2 Research Motivation

In a paper machine, the water drained from the wire is collected and recirculated through a complex distribution network in order to minimize the loss of valuable fiber, the effluent volume and the fresh water usage [11]. The water and its reuse influence stock proportioning, stock blending and consistency control of stock fed to the machine. Even fairly small changes in machine inlet flow can disturb the process performance and affect the final product quality. For this reason, the mixing point of the thick stock from the basis weight valve and the white water should be carefully designed and controlled to prevent consistency variations. Consistency variations or flow variations at the headbox slice affect *basis weight*, which refers to the mass of fibers per unit area of the sheet, and other paper properties. Maintaining constant quality of the stock fed to the headbox is an important factor in white water system design.

Most of the work over the past few decades concerning white water dynamics has focused on the development of heuristics from simulation results. In the system design, usually a number of storage tanks were incorporated in the white water system to dampen the effects of production disturbances such as paper machine breaks and production or grade changes. Even in well-designed systems, due to the white water recycles from different stages, such disturbances can cause significant variations in the consistency of the stock fed to the machine. This in turn will affect paper machine performance and the properties of the paper produced. Although individual units in paper machines can be well modelled, the overall system with white water recycle can exhibit much more complicated dynamics. On-line identification and adaptive control become an issue in the improvement of the design and control of this complex recycle system.

1.3 Thesis Outline

Chapter 2 models the white water recirculation system based on industrial specifications. Open loop dynamics is analysed. Some intrinsic phenomena that occur in this system are highlighted and summarized. Chapter 3 discusses the on-line estimation of the white water recycle system dynamics based on Laguerre series representation. Laguerre functions and recursive least-squares estimation algorithm are described with the discussion on the choice of the optimum Laguerre filter time scale. it is concluded with simulation results. In chapter 4, an adaptive generalized predictive controller is designed based on a state space form Laguerre model. The robustness of this control scheme is discussed along with a summary of the choice of the control system design parameters. Finally, the simulation results are discussed. Chapter 5 summarizes the results and contributions of this thesis with a discussion on future work that may lead to more improvement in this area.

Chapter 2

Process Analysis

This chapter describes the process modelling, and explores the dynamic characteristics which exist in the white water recycle system. Firstly, a wet-end revolution - consistency measurement under the wire is introduced. Then the model for each individual unit involved in the white water system is derived, based on mass balance equations. After that, the complete system model is set up to illustrate some interesting phenomena caused by the white water recirculation. Finally, a linearized system model is used to demonstrate the effects of various system parameters of the individual units to the overall recycling system performance.

2.1 Consistency Measurement under the Wire

In recent years, some paper mills in Europe have learned the benefits of measuring and controlling stock consistency on the forming wire by scanning the consistency gauge under the wire. But this is still a new concept in North America . To pave the way in putting this technology into practical use in North America, this thesis analyzes the wet web consistency control with the presence of white water recycle.

In order to get the consistency measurement on the wet web, some European mills mounted a gamma gauge in a fixed position under the wire. They measure stock mass and calculate consistency based on known dry weight of the sheet [23, 24, 25]. The scanner provides excellent weight profile information. It can be directed to scan just the edges, the full web width or any part of the sheet at designated intervals. The scanning gauge can show potential runability problems coming from the wire, provide immediate knowledge of forming section operation and expose wet-end problems early. By using this technology, the paper machine runability, sheet formation and product quality can be improved.

Forming section scanning offers new opportunities for analyzing paper machine variation. Since even small machine and web changes can cause web breaks and product quality problems, the consistency measurements are important in troubleshooting breaks. Apparently, the wire section is more critical then the press section in improving runability and throughput. In the following sections, the wet web consistency is considered as measured output in the system analysis.

2.2 Process Model

In this section, the modeling of the white water system, depicted on figure 2.2, is considered. Here, the system is technically defined as five major dynamic units: fan pump, a combination of cleaners, deaerator and screens, headbox, wire section and wire pit. The model for each individual part can be derived based on the principle of mass balance. The variables connecting the units represent mass transfers from one unit to another. The thick stock flowrate Q_s is the input variable. The stock with consistency C_s is added to the system. Then it is diluted with the white water (Q_w, C_w), and also mixed with the circulation flows from the headbox (Q_h, C_j) and the combination of cleaners, deaerator and screens (Q_r, C_l). White water also flows into the cleaners at the flowrate (Q_{dw}) to dilute the rejects. After those processing procedures, the stock is transported to the headbox at flowrate Q_l and consistency C_l. Out of the open slice of the headbox is the stock at the flowrate Q_j with consistency C_j. Most of the fibre in the stock is carried by the wires to the press section, while the liquid drained from the bottom wire is collected to the wire pit at flowrate Q with fibre consistency C. There is an overflow (Q_o, C_w) from the wire pit for maintaining the water level of the wire pit to avoid disturbances caused by head fluctuations. At the end of the wire section, the stock goes to the next stage, i.e. the press section, at flowrate Q_p. System output is the wet web stock consistency C_p. Without loss of generality, the system is modelled based on the following assumptions and simplifications.

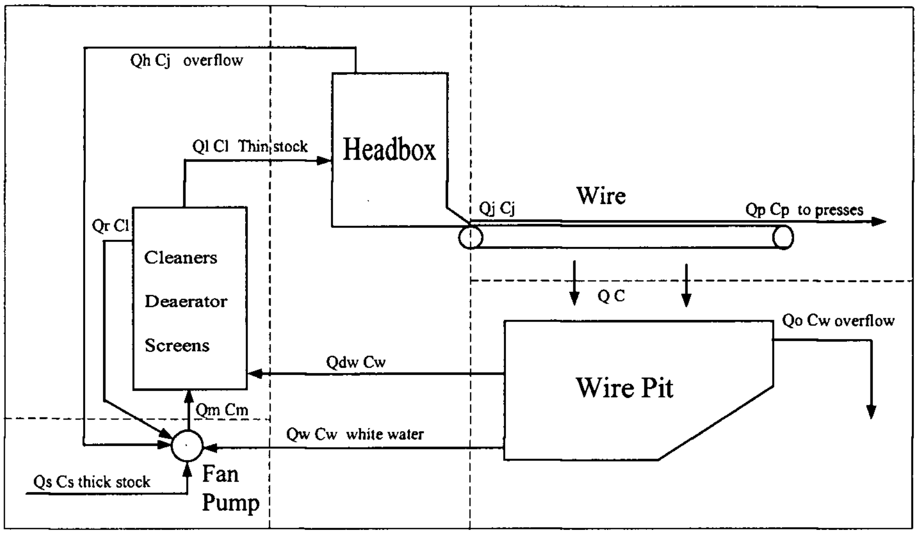

Figure 2.2: The Schematic diagram of white water system

- The white water from the wire section enters the wire pit and moves down with mixing and plug flow. The other recirculation flows that come into the bottom of the wire pit are assumed not to be mixed with the white water in the volume above. Instead these flows are inputs to the fan pump, where mixing takes place.

- Cleaners, deaerator and screens are considered as ideal mixing transportation pipe causing time delay only.

- The flow rate from deaerator to screens is constant (there is a fixed pump between them). As a result, the flow rate from screens to the headbox (Q_l) is constant.

- The output stock flowrate of the headbox (Q_j) is constant. Ideal mixing exists in the whole volume of the headbox.

- The output flowrate of the fan pump (Q_m) is kept constant.

2.2.1 Fan Pump

The fan pump can be modelled as a unit, with negligible volume, where instantaneous mixing of different flows occurs. It is assumed that the flows entering the bottom of the wire pit are mixed in the fan pump. The mass balance equation for the fan pump can be written as:

$$Q_m(t)C_m(t) = Q_s(t)C_s(t) + Q_w(t)C_w(t) + Q_r(t)C_l(t) + Q_h(t)C_j(t) \tag{2.1}$$

2.2.2 Cleaners, Deaerator and Screens

The cleaners are hydrocyclones where heavy dirt particles in the stock are seperated from the lighter fibers with the help of centrifugal forces. Then the stock goes to deaerator where air bubbles in the stock are removed. When the stock passes through the screens, flocculated fibres and other unexpected particles which could cause problems in the machine are filtered out and removed. Except the mainstream of the stock, there is another outlet in the deaerator for recirculating the overflow to the wire pit. The rejects from cleaners and screens are discharged to a sewage system. Comparing with the mainstream, the rejects only contain few fibres, therefore their effects to the mainstream stock consistency can be ignored in the system modeling. Neglecting consistency changes in the cleaners and screens and assuming that the white water used in the cleaners is ideally mixed with the stock at the inlet point, the dynamics for the cleaners, deaerator and screens can be simplified as a pure transport delay as follows:

$$C_{out}(t) = C_{in}(t - T_f) \tag{2.2}$$

where C_{out} and C_{in} are outlet and inlet consistencies respectively. T_f is the transport delay. The outlet consistency C_{out} is thin stock consistency C_l, and the inlet consistency C_{in} can be derived from both input flows.

2.2.3 Headbox

A hydraulic design of headbox is considered in this system. The main task for the headbox is to distribute the stock across the wire of paper machine. The discharge velocity from the open slice depends directly on the pressure at the slice. There is an overflow channel located in the opposite side of the inlet. It is assumed that ideal mixing is achieved in the whole volume of the headbox. The model then becomes an ideal mixing tank with the equation:

$$V_h \frac{dC_j(t)}{dt} = Q_l(t)C_l(t) - (Q_h(t) + Q_j(t))C_j(t) \tag{2.3}$$

where the headbox volume V_h is constant.

2.2.4 Wire Section

As the sheet forms, some fibres go through the wire with the white water, while most of them stay on and are carried by the wire to the press section. The amount of the fibres that stay on the wire at the presses is characterized by a factor called *first pass retention* or just *retention.* Neglecting the transportation time from the slice to press section(generally a couple of seconds), the retention R is a function of the basis weight and is defined as:

$$R = \frac{Q_p(t)C_p(t)}{Q_j(t)C_j(t)} \tag{2.4}$$

2.2.5 Wire Pit

Into the wire pit comes the white water drained from the wire section and also some other recirculation flows from other units in the white water system. It is assumed that those recirculation flows run into the fan pump directly without mixing with the white water in the wire pit, therefore those flows are not taken into account here but in the fan pump. The wire pit can be modelled as a tank with mixing and plug flow. The mass balance equation for the wire pit is:

$$V_w \frac{dC_w(t)}{dt} = Q(t)C(t - T_r) - (Q_{dw}(t) + Q_w(t) + Q_0(t))C_w(t) \tag{2.5}$$

where the wire pit volume V_w is constant. T_r is the transportation delay caused by the plug flow in the wire pit.

2.2.6 The Complete System

The complete system model, shown in figure 2.3, is formed by combining all of above individual models together. The input to the model is the control signal to the thick stock valve. The summation here stands for the fan pump where the thick stock is mixed with the recycled white water and some other flows. The forward path consists of cleaners, deaerator, screens, headbox and wire section. The wire pit is in the recycle path. The transportation delay caused by cleaners, deaerator and screens exists in the forward path, so called forward path time delay T_f. A typical value is around 30 seconds. The time delay caused by the plug flow in the wire pit appears in the recycle route. The recycle path time delay T_r can be calculated from the wire pit physical size.

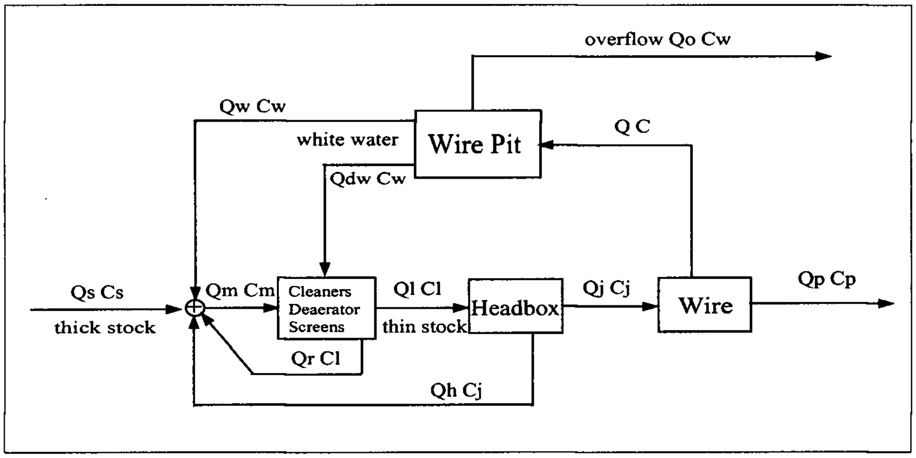

Figure 2.3: White water system block diagram

2.3 System Dynamics

2.3.1 System Simulator

MATLAB SIMULINK is chosen for the system modelling and simulation. The complete white water recycle system simulation model is illustrated in figure 2.4 in which the output of the model is the wet web consistency before the press section and the input is the thick stock flowrate. The design parameters in the model equations in Section 2.2 are obtained from an existing fine paper machine as listed below:

System Design Parameters:

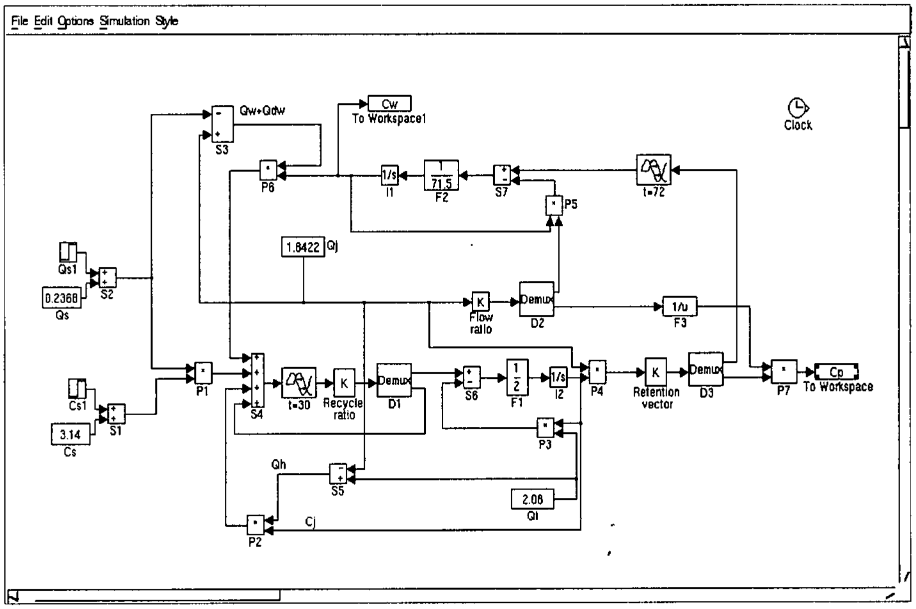

Figure 2.4: White water system simulation diagram

- Wire pit

  Diameter: $D = 3m$

  Height: $H = 10.65m$

  Liquid level: $L = 90\%$

  Plug flow height: $H_1 = 7.65m$

- Headbox

  Volume: $V = 2(m^3)$

System Parameters:

Retention :	$R = 0.75$
Recycle ratio :	$0.3549 : 0.6451$
Flow ratio :	$0.979 : 0.021$
Thick stock :	$Q_s = 0.2368\ m^3/s \quad C_s = 3.14\%$
Thin stock :	$Q_l = 2.08\ m^3/s$
White water :	$Q_w = 0.756\ m^3/s$
Drainage water :	$Q = 1.697\ m^3/s$
Stock out of the headbox :	$Q_j = 1.842\ m^3/s$
Forward path time delay :	$T_f = 30secs$
Recycle path time delay :	$T_r = 72secs$

The major objective in this study of the white water recycle system is to explore the effect of the white water recirculation stream on the overall system performance. Therefore accurate cleaners, deaerator, screens and drainage models are not necessary. The recycle ratio, flow ratio and retention are used to describe the dynamics of those units without loss of generality. The recycle ratio is defined as the mass recycle ratio from the cleaners, deaerator and screens to the wire pit $(Q_r C_l / Q_l C_l)$, and the flow ratio is the flow recycle ratio from the open slice of the headbox to the wire pit (Q/Q_p).

Step responses

The step response of a system is commonly used to illustrate process dynamics. Figure 2.5 shows the step responses of wet web consistency and white water consistency with and without recycle from the wire pit. The bump test here was performed by making a step change in the control signal to the thick stock valve. The thick stock at a consistency of 3.14 % is inputed to the system, and a step change of the thick stock flowrate is made from value 0.2368 m^3/s to 0.2568 m^3/s at time $t = 0$.

The initial bumps in wet web consistency responses are caused by the short recirculations

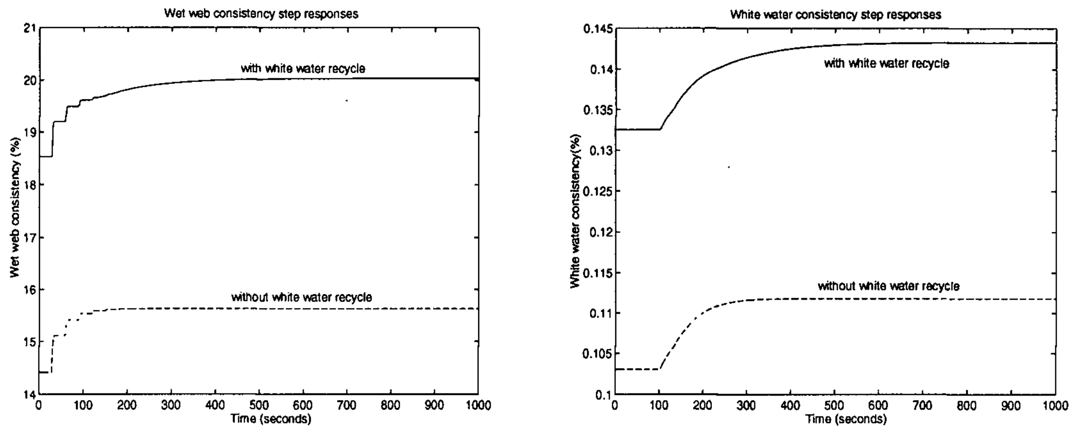

Figure 2.5: Open-loop step test results

from headbox, deaerator and screens. The time delay in the forward path makes the output value periodically increase at the interval of $T_f(30ssecs)$ with decreasing amplitudes. The white water consistency response exhibits a delay of 102 seconds $(T_f + Tr)$ and somewhat first order dynamic behaviour. Since the white water returns to the original stage of the process, its dynamics starts affecting the wet web consistency after another 30 seconds (T_f-forward path time delay). The effect of the recycle stream increases the steady state value of wet web consistency. If there is no white water recycling from wire pit, and instead an equivalent amount of fresh water is supplied to dilute the stock, the wet end consistency reaches a smaller steady state value in a shorter time (see the dashed line). Obviously, the recycle increases the steady state gain and the time constant of the process.

Impulse responses

Some interesting features that are peculiar to recycle systems can be better revealed by observing the impulse responses. There are two ways to get the impulse response for the white water recycle system. One is by differentiating the step response, and the other is to simulate the response by using an impulse input to the system. Figure 2.6 is the wet web consistency impulse response obtained by differentiating the step response in the previous part. The figure

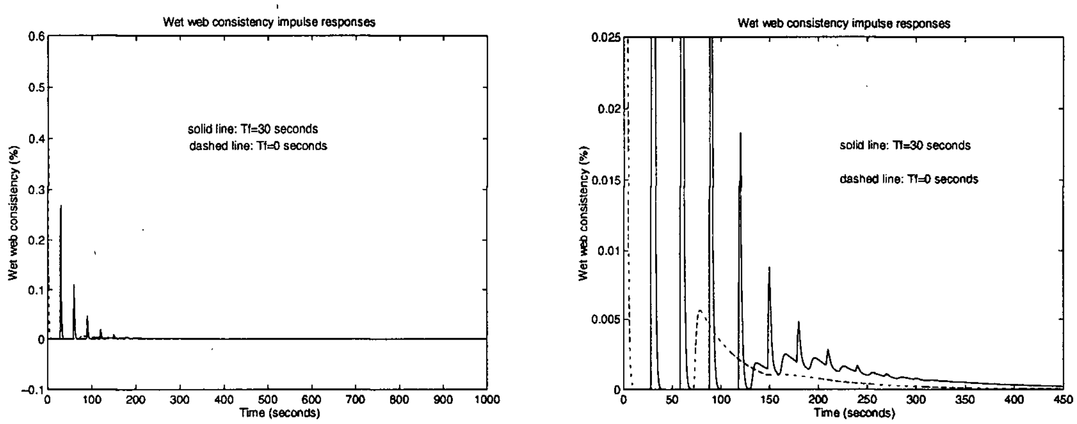

Figure 2.6: Wet web consistency impulse response

on the right hand side is the same impulse responses as the left one with an enlarged scale, so as to achieve a clear image of the white water recycle stream. In the response of the system with forward path time delay (see the solid line), the first pulse is caused by the impulse input signal, while the subsequent pulses appeared at the interval of the forward path time delay (T_f) are contributed by the circulations from the headbox, deaerator and screens. They are dampened with time because those circulation variables gradually approach their steady state values. At the same time, the effect of the white water recycle starts to appear in the wet web consistency after 132 seconds, i.e. twice of the forward path delay plus recycle delay. It can be clearly seen from the block diagram that the stock goes through the forward path, then part of it recirculates to the original stage of the process through the recycle route, and goes through the forward path once again before it reaches the end of the wire section. The impulse response of the white water recycle system exhibits unique dynamics. Except for the first pulse, the inner recirculation loops produce a series of subsequent pulses with decreasing amplitudes. The white water recycle triggers another transient with longer time delay and larger time constant. The latter can be clearly seen in the response without transportation delay from the fan pump to the headbox (see the dashed line in the right-hand side of figure 2.6).

The white water consistency impulse responses exhibit similar phenomena as shown in Figure 2.7. Some pulses with the same period (T_f) exist in the response, which are induced by the short circulations. If there is no time delay in the forward path, the response is free of those pulses, and it reacts faster and stronger to the impulse input (see the dashed line in figure 2.7). From the above discussion, it is clear that the white water recycle changes not only the steady state characteristics, but also transient dynamics.

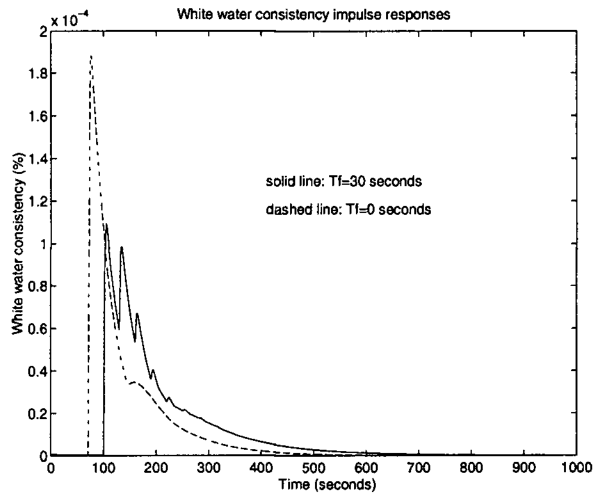

Figure 2.7: White water consistency impulse response

2.3.2 System Characteristics

Every individual unit contributes differently to the overall process dynamics. The headbox and wire pit play more important roles in the recycle system. This section attempts to study the contributions of individual units to the overall system performance. Thus simplified transfer function models (figure 2.8) are used to simulate the white water recycle system responses for various parameters of individual units. To linearize the system, the overflows from the headbox and deaerator are neglected. All the flow rates are kept constant except the thick stock flow rate. The transfer function of each unit is derived from mass balance equations in Section 2.2. The mass balance equation for the headbox is

$$V_h \frac{dC_j(t)}{dt} = Q_l C_l(t) - Q_j C_j(t) \tag{2.6}$$

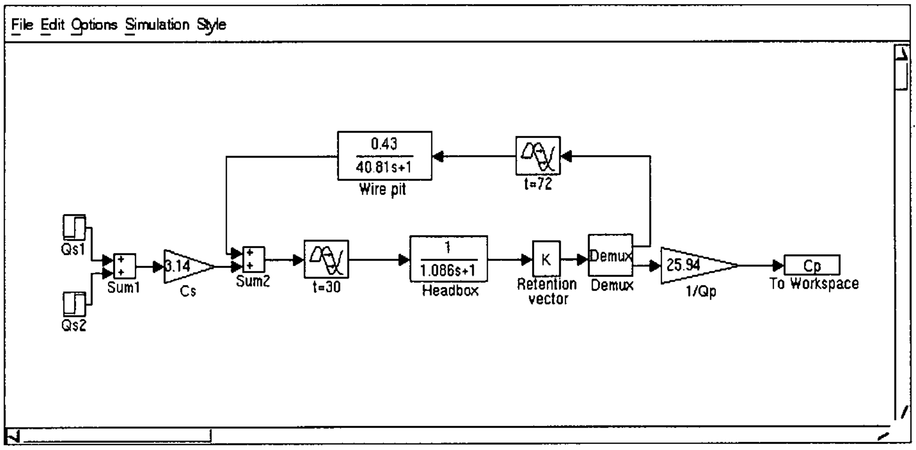

Figure 2.8: Linearized system simulation diagram

Multiplying Q_j on both sides of equation 2.6, it becomes

$$V_h \frac{dQ_jC_j(t)}{dt} = Q_j(Q_lC_l(t) - Q_jC_j(t)) \tag{2.7}$$

Here, the mass out of the headbox $(Q_jC_j(t))$ is considered as the output variable and the mass into the headbox $(Q_lC_l(t))$ is the input variable. The values of V_h and Q_j are given in section 2.3.1, therefore the headbox transfer function $G_h(s)$ is obtained as follows:

$$G_h(s) = \frac{1}{1.086s+1} \tag{2.8}$$

The wire pit mass balance equation is given in the form of

$$V_w \frac{dC_w(t)}{dt} = QC(t-T_r) - (Q_{dw} + Q_w + Q_0)C_w(t) \tag{2.9}$$

Multiplying by Q_w, and consider

$$Q = Q_{dw} + Q_w + Q_0 \tag{2.10}$$

then

$$V_w \frac{dQ_wC_w(t)}{dt} = Q_wQC(t-T_r) - QQ_wC_w(t) \tag{2.11}$$

with input $QC(t)$ and output Q_wC_w and other variable data in section 2.3.1, the wire pit transfer function $G_w(s)$ is given as

$$G_w(s) = \frac{0.43e^{-72s}}{40.81s+1} \tag{2.12}$$

The forward path time delay here stands for the transportation delay in the cleaners, deaerator and screens. The headbox is modelled as a ideal mixing tank with first order dynamics with time constant $\tau_h = 1.086(secs)$. While the wire pit is a mixing tank with plug flow, its model consists of a steady state gain$K_r = 0.43$, a first order lag with time constant $\tau_w = 40.81(secs)$ and time delay $T_r = 72(secs)$. The stock separates into two streams at the wire. It can be simply described by the retention vector. Again, a step change of the thick stock flowrate is made from value 0.2368 to 0.2568 at time $t = 0$ for the following simulations.

Wire pit time constant

The wire pit is located in the recycle path. Theoretically, the wire pit time constant would affect recycle dynamics. The simulation results are shown in figure 2.9 for three different wire pit time constant values (τ_w =20.81, 40.81 and 80.81). The retention is set to be 0.75 in these simulations.

The wet web consistency responses illustrate that the wire pit time constant only affects the transient response of the recycle stream. That merely causes slight effect on the overall system performance. A small recycle time constant, equivalent to a smaller volume of the wire pit , is expected to achieve faster recycle response. However the system would be sensitive to load disturbance if the volume of the wire pit is too small. Therefore the trade-off between recycle response speed and system disturbance rejection should be considered for the system design.

Retention

Retention determines the amount of fibres that stay on the wire at the point of the end of the wire section. It is clear that the higher the retention, the higher the wet web consistency, and the lower the white water consistency, see figure 2.10. A high retention is a goal to endeavor to achieve in industry in order to make efficient use of fibres.

Various time delays of individual units

The time delay in the forward path is the transportation delay from the fan pump to the headbox. Figure 2.11 confirms the results obtained in the system step and impulse responses in Section 2.3.1. The forward path time delay affects the recycle stream twice as much as the forward stream.

Actually, the time delay in the wire pit is related to its volume. When the volume decreases, both the time constant and time delay would decrease, and vice versa. The wet web consistency responses in Figure 2.12 show that this time delay has effect only on the recycle stream.

2.3.3 Conclusions

When recycling exists in a process, the dynamics become much more complicated. In the white water recycle system, various recycle flows recirculate to the fan pump from different stages of the process. These recycle streams make a noticeable impact on system performance. Typically, recycling increases system time constant and steady state gain.

Every individual unit in the recycle system would affect the overall process dynamics. The simplified transfer function models have been used to reveal the effects of various parameters of the individual units in the white water recycle system. The time constant and the time delay in the recycle path only affect the dynamics of the recycle stream. However, the time delay in the forward path has strong impact on both forward flow and recycle flow behaviors. The forward path is the only route to reach the system output point. Especially, the flow recycled from the wire section must pass through the forward path one more time before it reaches to the end of the wire section. Therefore this parameter affects the recycle flow twice as much as they do to the forward flow.

Retention is an important parameter governing the amount of the fibres that stay on the wire. The higher the retention, the higher the wet web consistency, and the lower the white water consistency.

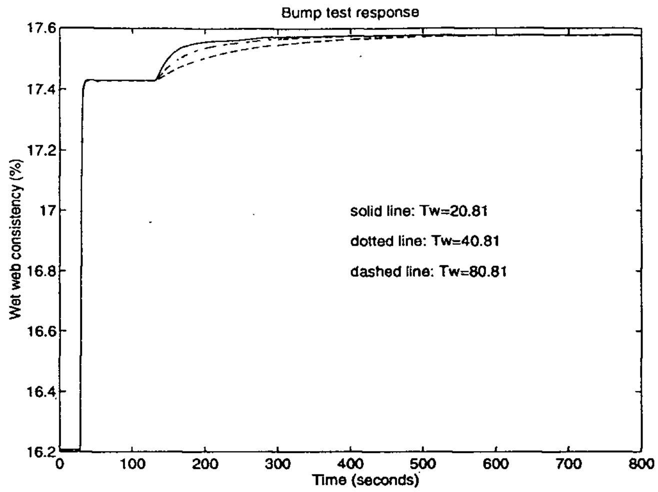

Figure 2.9: Bump tests for different wire pit time constants

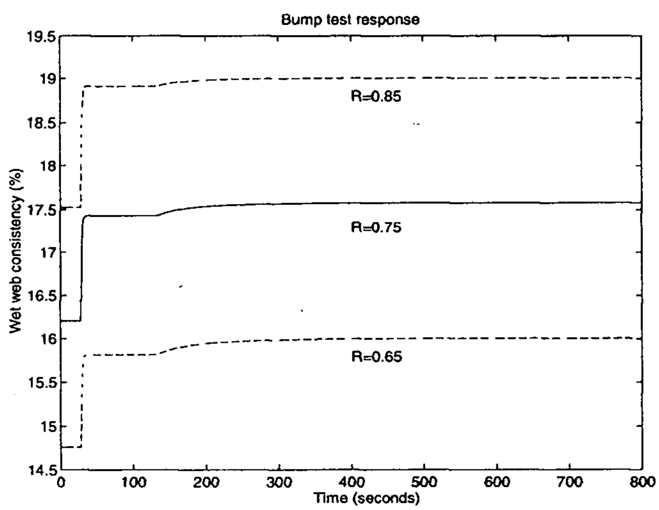

Figure 2.10: Bump tests for different retentions

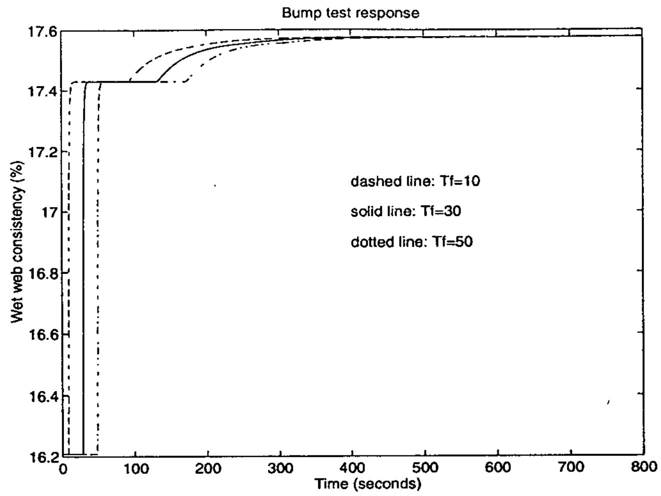

Figure 2.11: Bump tests for different forward path time delays

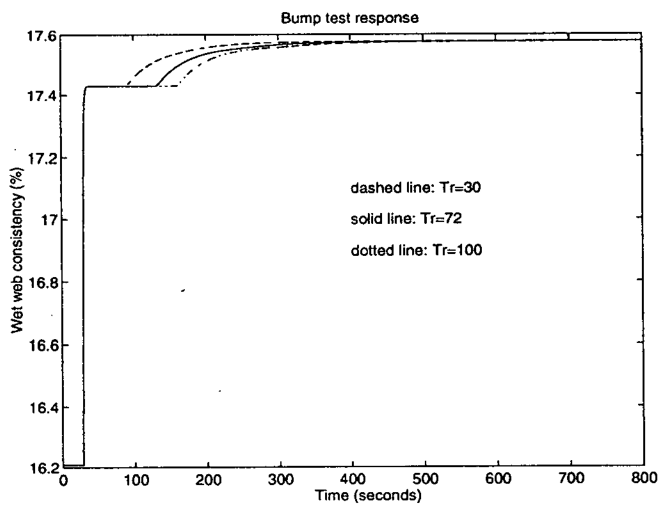

Figure 2.12: Bump tests for different recycle path time delays

Chapter 3

System Identification

This chapter discusses the use of Laguerre filter based models to represent the dynamics of the white water recycle system for on-line identification. First, some background on the use of orthonormal functions as a modelling tool for process dynamic representations is given. Then the Laguerre series representation and recursive least-squares estimation algorithm are described. The chapter ends with the discussion on the choice of the Laguerre filter time scale and system simulation results.

3.1 Background

An analysis of the system response can generate much of the information required for system identification. A good model of the white water system is required for improving the control of paper machine. Over the past few decades, most of the work concerning white water dynamics has focused on the development of heuristics from simulation results. While these simulations were based on simplified simulation models under certain assumptions at the expense of some inaccuracy, there is no easy way to obtain a transfer function form model of the white water recycle system to describe the process operation. Thus on-line determination of process dynamics becomes an issue. One of the key elements of system identification is the selection of a mathematical model representation. During the last two decades, research on the use of orthonormal functions to represent the dynamics of processes for system identification has achieved great successes. An orthonormal series representation is a good choice as a modeling tool for stable plants without structural knowledge. In the white water recycle system, different time delays exist in the forward path, recycle path and other units. In this thesis, the Laguerre series representation is chosen for system modeling because of its simplicity and strong features in identifying models with uncertain or long time delays.

The major advantage in using Laguerre function based models is that any stable plant can be modelled without accurate knowledge of the true plant model structure, such as the plant order and time delay. Because the set of Laguerre functions is similar to *Padé* approximants, it is extremely effective in representing system time delays. The resulting model is robust to time delay variations and valuable for processes with long time delays. In the early 1980's, the use of Laguerre functions to represent process dynamics was proposed for system identification and adaptive control. This work led to the successful development of several types of adaptive control schemes and their applications in industry. Dumont and Zervos (1986) proposed an unstructured adaptive predictive controller using a Laguerre function based model[16]. Simulation results showed that this control scheme is a robust and simple-to-use algorithm that requires minimal a priori information. In 1988, they presented a new stochastic self-tuning controller with both the physical plant and stochastic noise modelled by Laguerre series representations[18]. It was proved to be robust, not sensitive to the initial parameter settings and capable of producing good control. They also extended the single-input single-output Laguerre function based adaptive control algorithms to the multivariable case to overcome the difficulty in the representation of time delays of MIMO systems by a delay matrix (1988) [19]. Furthermore Dumont et al. (1990) [20] applied the self-tuning scheme based on the orthonormal Laguerre functions on a real industrial plant. The new self-tuner provided better control of a pH loop exhibiting a large and variable dead-time. One way of choosing the Laguerre time scale that provides rapid convergence of the Laguerre spectrum has been discussed by Dumont et al.(1991) [21]. In that paper, several Laguerre function based adaptive control algorithms were developed. Elshafei et al. (1994) studied the robustness and stability of adaptive generalized predictive controller (GPC) based on Laguerre-filters to handle severe unstructured uncertainties[22]. It was proved that the Laguerre-filter-based model is superior for high-order, overdamped and time-delay systems. This is a direct consequence of its simple filter ladder network form as described in the following section.

3.2 Laguerre Functions

The use of orthogonal functions for obtaining approximations can be traced back to the development of Fourier series. Although the Fourier series is the most commonly used orthogonal series representation, there are many other orthogonal functions, which may be more suitable for a particular situation. The Laguerre functions have a special significance in the transient problem, because they can be constructed in a relatively simple linear filter form with finite order. In continuous time, the Laguerre functions are described by

$$l_i(t) = \sqrt{2p}\frac{e^{pt}}{(i-1)!}\frac{d^{i-1}}{dt^{i-1}}[t^{i-1}e^{-2pt}] \tag{3.13}$$

where i is the order of the function($i = 1, ..., N$) and p is the time scale. These functions form an orthogonal set in the time-domain $[0, \infty)$. In Laplace transform domain, the Laguerre filters are written in the form

$$L_i(s) = \sqrt{2p}\,\frac{(s-p)^{i-1}}{(s+p)^i} \tag{3.14}$$

Laguerre filters are readily implemented by a simple and convenient ladder network (see figure 3.13). The network consists of a chain of identical pure phase-shift filters and a first order low pass filter. The Laguerre-filters-based model can also be expressed in a stable, observable

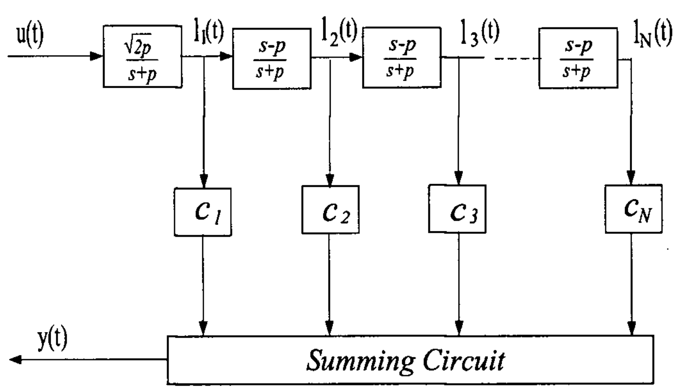

Figure 3.13: Laguerre ladder network

and controllable discrete-time state-space form [22]. Based on the state-space form, predictive expressions of system outputs can be derived in a straightforward manner. The outputs from each block are taken as the states of the Laguerre ladder network:

$$\boldsymbol{l}^T(t) = [l_1(t)\ l_2(t) \dots l_N(t)] \tag{3.15}$$

By discretizing each block, the Laguerre-filter-based model in the discrete state space form can be written

$$\boldsymbol{l}(t+1) = A\boldsymbol{l}(t) + \boldsymbol{b}u(t) \tag{3.16}$$

$$y(t) = \boldsymbol{c}^T \boldsymbol{l}(t) \tag{3.17}$$

The output of the Laguerre model is obtained by the weighted summation of the outputs of the Laguerre filters. Where, $u(t)$ is the system input and $y(t)$ is the system output. A is a lower triangular $N \times N$ matrix where the same elements are found respectively across the diagonal and every sub-diagonal.

$$A = \begin{bmatrix} \tau_1 & 0 & \cdots & 0 \\ \frac{-\tau_1\tau_2-\tau_3}{T_s} & \tau_1 & \cdots & 0 \\ \vdots & \ddots & \ddots & \vdots \\ \frac{(-1)^{N-1}\tau_2^{N-2}(\tau_1\tau_2+\tau_3)}{T_s^{N-1}} & \cdots & \frac{-\tau_1\tau_2-\tau_3}{T_s} & \tau_1 \end{bmatrix} \tag{3.18}$$

$$\boldsymbol{b}^T = \begin{bmatrix} \tau_4 & \frac{-\tau_2}{T_s}\tau_4 & \cdots & \left(\frac{-\tau_2}{T_s}\right)^{N-1}\tau_4 \end{bmatrix} \tag{3.19}$$

$$\boldsymbol{c}^T = [c_1\ c_2 \dots c_N] \tag{3.20}$$

The constants τ_1, τ_2, τ_3 and τ_4 are given in terms of the sampling period T_s and the Laguerre time scale p as

$$\tau_1 = e^{-pT_s} \tag{3.21}$$

$$\tau_2 = T_s + \frac{2}{p}(e^{-pT_s} - 1) \tag{3.22}$$

$$\tau_3 = -T_s e^{-pT_s} - \frac{2}{p}(e^{-pT_s} - 1) \tag{3.23}$$

$$\tau_4 = \sqrt{2p}\frac{(1-\tau_1)}{p} \tag{3.24}$$

The constants in the vector $\boldsymbol{c}$ are called Laguerre spectrum gains. Least squares parameter estimation can be effectively used for on-line identification.

3.3 Recursive Least-Squares Estimation

The least-squares method is widely used for parameter estimation. The least-squares estimate can be calculated analytically if the model is linear in the parameters. As described above, any stable system can be exactly expressed by an infinite Laguerre series representation. In practice, only a truncated form is used to obtain an approximate process model. A more accurate model could be achieved by increasing the order of Laguerre functions. The coefficients of lower order terms can be precisely estimated by using least-squares parameter estimation, while the higher order coefficients tend to zero. In its discrete-time state space form, the output is a linear function of the state vector as follows:

$$y(t) = \boldsymbol{c}^T \boldsymbol{l}(t) \tag{3.25}$$

The least-squares method is particularly simple for a mathematical model in the above form, where $\boldsymbol{c}$ is the Laguerre coefficient vector which needs to be determined, and $\boldsymbol{l}(\mathrm{t})$ is the state vector of the Laguerre filters. The problem is to determine the parameters so that the difference between the model outputs and the plant outputs is minimized in the least squares sense. Introducing the following notations:

$$\boldsymbol{\phi}^T(k) = [l_1(k)\ l_2(k) \ldots l_N(k)] \tag{3.26}$$

$$\boldsymbol{\theta} = [c_1\ c_2 \ldots c_N]^T \tag{3.27}$$

$$\boldsymbol{Y}(\mathrm{t}) = [y(1)\ y(2) \ldots y(t)]^T \tag{3.28}$$

$$\boldsymbol{\Phi}(\mathrm{t}) = [\boldsymbol{\phi}^T(1)\ \boldsymbol{\phi}^T(2) \ldots \boldsymbol{\phi}^T(t)]^T \tag{3.29}$$

where k often denotes sampling time, one can write

$$\boldsymbol{Y} = \boldsymbol{\Phi}^T \boldsymbol{\theta} \tag{3.30}$$

The parameter vector should be chosen to minimize the least-squares loss function

$$V(\theta, t) = \frac{1}{2}\sum_{i=1}^{t}(y(i) - \phi^T(i)\theta)^2 \tag{3.31}$$

The least-squares estimate of Laguerre coefficients [27] is then given by

$$\hat{\theta} = (\Phi^T\Phi)^{-1}\Phi^T Y \tag{3.32}$$

Define the inverse of the covariance matrix:

$$\boldsymbol{P}(t) = (\boldsymbol{\Phi}^T(t)\boldsymbol{\Phi}(\mathrm{t}))^{-1} \tag{3.33}$$

The recursive least-squares estimate $\hat{\theta}(t)$ can be obtained by using the following equations

$$\hat{\boldsymbol{\theta}}(t) = \hat{\boldsymbol{\theta}}(t-1) + K(t)(y(t) - \boldsymbol{\phi}^T(t)\hat{\boldsymbol{\theta}}(t-1)) \tag{3.34}$$

$$K(t) = \boldsymbol{P}(t-1)\phi(t)(\ \boldsymbol{I} + \boldsymbol{\phi}^T(t)\ \boldsymbol{P}(t-1)\phi(t))^{-1} \tag{3.35}$$

$$\boldsymbol{P}(t) = (\ \boldsymbol{I} - K(t)\boldsymbol{\phi}^T(t))\ \boldsymbol{P}(t-1) \tag{3.36}$$

Equation (3.34) intuitively shows that the estimate $\hat{\theta}(t)$ is calculated by making a correction to the previous estimate $\hat{\theta}(t-1)$. $K(t)$ is the weighting vector, thus the correction is proportional to the difference between the measured output and the output predicted based on the previous parameter estimate.

The matrix $P(t)$ is defined only when the matrix $\Phi^T(t)\Phi(t)$ is nonsingular. It is assumed that the matrix $\Phi(t)$ has full rank, i.e. $\Phi^T(t)\Phi(t)$ is nonsingular for $t \geq t_0$. To obtain an initial condition for P, it is necessary to choose $t = t_0$, then

$$\boldsymbol{P}(t_0) = (\boldsymbol{\Phi}^T(t_0)\boldsymbol{\Phi}(t_0))^{-1} \tag{3.37}$$

$$\hat{\boldsymbol{\theta}}(t_0) = \boldsymbol{P}(t_0)\boldsymbol{\Phi}^T(t_0)\ \boldsymbol{Y}(t_0) \tag{3.38}$$

Usually, it is convenient to use the recursive equations in all steps. If the recursive estimation is started with the initial condition

$$\boldsymbol{P}(0) = \boldsymbol{P}_0 \tag{3.39}$$

where P_0 is positive definite, then

$$\boldsymbol{P}(t) \;=\; (\,\boldsymbol{P}_0^{-1} + \boldsymbol{\Phi}^T(t)\boldsymbol{\Phi}(t))^{-1} \tag{3.40}$$

Now, $P(t)$ can be made close to $(\Phi^T(t)\Phi(t))^{-1}$ by choosing a sufficient large P_0. A common choice of initial values for recursive parameter estimation is

$$\boldsymbol{P}(0) \;=\; R\,\boldsymbol{I} \tag{3.41}$$

$$\boldsymbol{\theta}(0) \;=\; 0 \tag{3.42}$$

where R is a large scalar.

In the next section, the recursive least-squares method is used to estimate Laguerre coefficients in the white water recycle system models. The initial condition $R = 1000$ is used in the following simulations.

3.4 Identification Results

3.4.1 Choice of Time Scale

Theoretically speaking, an infinite Laguerre series can be used to exactly represent a stable system. In practice, a truncated one is used instead. For a given system, the truncation error is function of the number of Laguerre filters and their time scale. For a fixed number of filters, there exists an optimal time scale that minimizes the error and lets the coefficients of higher order Laguerre functions tend to zero quickly. Then the problem of how to find the optimal time scale comes up. An optimum choice of the time scale for discrete Laguerre network was discussed by Fu and Dumont, 1993 [28]. This optimization algorithm is based on the minimization of the performance index:

$$J = \sum_{i=1}^{\infty} i g_i^2 \tag{3.43}$$

for the discrete Laguerre functions defined in z-domain as:

$$L_i(z) = \frac{\sqrt{1-a^2}}{z-a}\,(\frac{1-az}{z-a})^{i-1} \tag{3.44}$$

where a is the time scale of this Laguerre function and g_i ($i = 1, 2, 3, \ldots$) are called Laguerre coefficients. The performance index linearly increases the weighting of each additional Laguerre coefficient. As a result, a fast convergence rate can be obtained when the minimum is achieved. This is important for improving the match between a real plant and its model when a truncated Laguerre representation is used to model the plant dynamics. The optimal time scale is derived by minimizing the performance index in equation (3.43)

$$a_o = \frac{2M_1 - 1 - M_2}{2M_1 - 1 + \sqrt{4M_1M_2 - M_2^2 - 2M_2}} \tag{3.45}$$

where M_1 and M_2 are defined as:

$$M_1 = \frac{1}{||h||^2} \sum_{n=0}^{\infty} nh^2(n) \tag{3.46}$$

$$M_2 = \frac{1}{||h||^2} \sum_{n=0}^{\infty} n[\triangle h(n)]^2 \tag{3.47}$$

and n is the sampling time, $h(n)$ is the impulse response of a discrete system which is given by

$$h(n) = \sum_{i=1}^{\infty} g_i l_i(n) \tag{3.48}$$

and

$$||h||^2 = \sum_{n=0}^{\infty} h^2(n) = \sum_{i=1}^{\infty} g_i^2 \tag{3.49}$$

M_1 and M_2 characterize the rate of decay and the smoothness of the impulse response of the process, and they are also affected by the time delay. From the above result, it can be seen that the optimal time scale depends on the characteristics of the system impulse response.

So far, there is no effective method to choose the order of the Laguerre function. Practically, the higher the order, the more accurate the model. But a balance between estimation error and calculation time needs to be reached. For a known optimal time scale, a reasonable number N can be chosen when the coefficient of the highest order is as close to zero as expected, and the estimation error remains under an acceptable value.

3.4.2 Simulations and Discussions

Models of the white water recycle system can be constructed based on the Laguerre representation described in the previous sections with the state-space form:

$$\boldsymbol{l}(t+1) = A\boldsymbol{l}(t) + \boldsymbol{b}u(t) \tag{3.50}$$

$$y(t) = \boldsymbol{c}^T\boldsymbol{l}(t) \tag{3.51}$$

where the matrix A and the vector b are given in terms of the sampling time and the Laguerre time scale as defined in equations (3.18) and (3.19). The sampling time of 1 second is chosen for the following simulations. The vector c is the Laguerre coefficient vector which has to be estimated on-line. The Laguerre time scale has a strong impact on the quality of the approximation and the convergence rate of the Laguerre coefficients, therefore searching for the optimum time scale is important for system modeling. By using the Laguerre toolbox, the optimum time scale can be found according to the discussion in section 3.4.1. The knowledge of the impulse response is required to get the searching solution. Figure 3.14 is the discrete impulse response of the white water recycle system. For a tolerable pole error of 0.0001, the

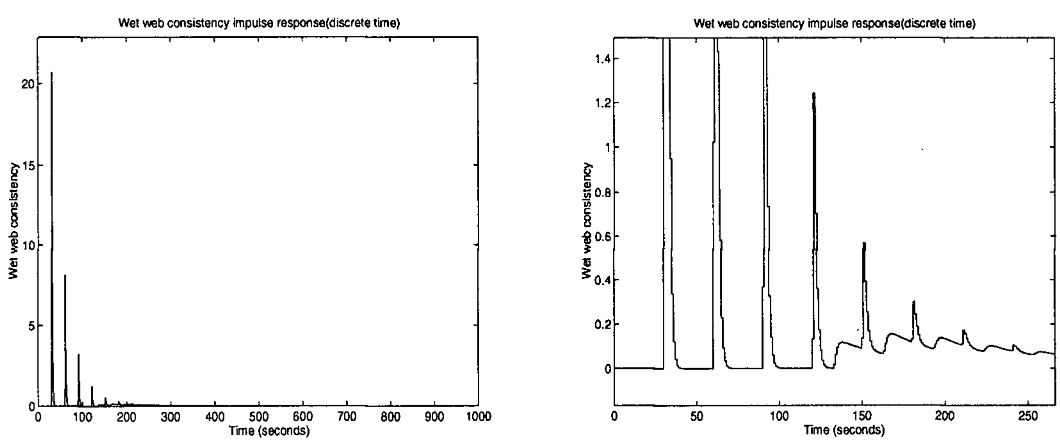

Figure 3.14: Discrete impulse response

searching results for different Laguerre filter number are shown in table 3.1.

With given order and the pole, the Laguerre model can be obtained by on-line estimation of the Laguerre filter coefficient vector via least-squares estimation algorithm. The properties of

order	pole	order	pole
5	0.9664	9	0.9627
6	0.9564	10	0.9559
7	0.9467	11	0.9607
8	0.9694	12	0.9420

Table 3.1: Optimum Laguerre Filter Poles

the input signal used in parameter estimation are crucial for the quality of the estimates. The parameters of the model cannot be identified unless some conditions are imposed on the input signal. In this section, the simulation is implemented in two steps. The first step is to make a step change on the input signal from 0 to 0.2368 at time $t = 0$ to see the transient response with the effect of the estimated coefficient convergence. After the system gets to the steady state, at time $t = 2000$ seconds another small step change on the input signal from 0.2368 to 0.2568 is used to see the identification result without the strong impact of the coefficient convergence. The simulation block diagram is shown in figure 3.15. In order to demonstrate the characteristics of Laguerre series representations and the influence of the Laguerre filter order on approximation accuracy, as an example, two typical orders ($N = 6$ and 12) are considered in following simulations.

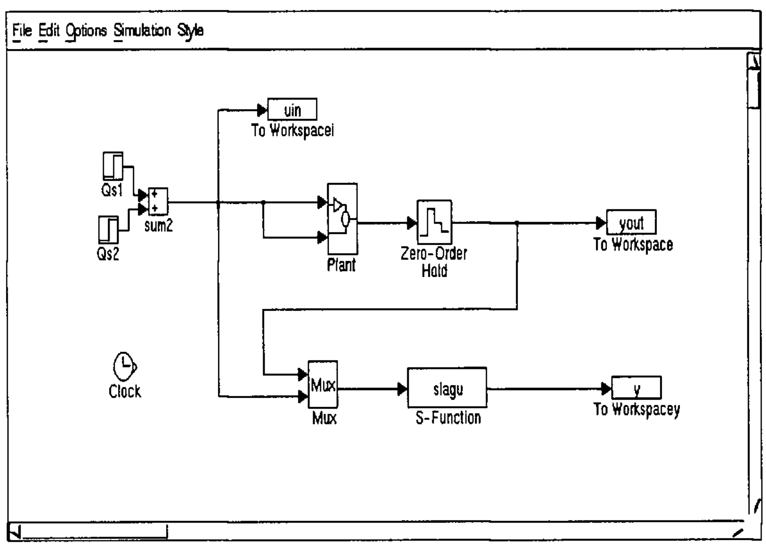

Figure 3.15: RLS parameter estimation simulation diagram

The input is imposed on the plant and the output is measured. Pairs of observation and input data are obtained from simulation and fed to the Laguerre model for the parameter estimation. A S-function is programmed to realize on-line estimation based on least-squares algorithm with the help of the Laguerre toolbox (see Appendix program 1). Figure 3.16 and 3.17 show the identification results for Laguerre filter order $N = 6$ and 12 respectively. These results illustrate that the Laguerre model is extremely effective in identifying a plant with significant time delay. Especially, for the white water recycle system, forward path and recycle path time delays occur in the different stage. All these delays clearly exhibit in the Laguerre model responses. By comparing these results, obviously, the higher order Laguerre model provides quicker convergence and better match with the real plant. This result can also be concluded from the integrated square errors calculated from $t = 2000$ seconds to 4000 seconds as shown in figure 3.18. To obtain a general knowledge of convergence speed of estimated coefficients, the estimated coefficients for a sixth order Laguerre model is shown in figure 3.19.

3.5 Conclusions

In this chapter the Laguerre function was used in the white water recycle system modelling. With on-line estimation of Laguerre coefficients by using recursive least-squares method, the resulting model with optimal Laguerre pole has achieved very good match with the plant. The simulation results have shown that the Laguerre model is extremely effective in identifying the time delays in the different stages of the white water recycle system. As expected, a higher order Laguerre model provides quicker convergence and better match with the real plant. It can be concluded that the Laguerre series representation is superior for the white water recycle system modelling.

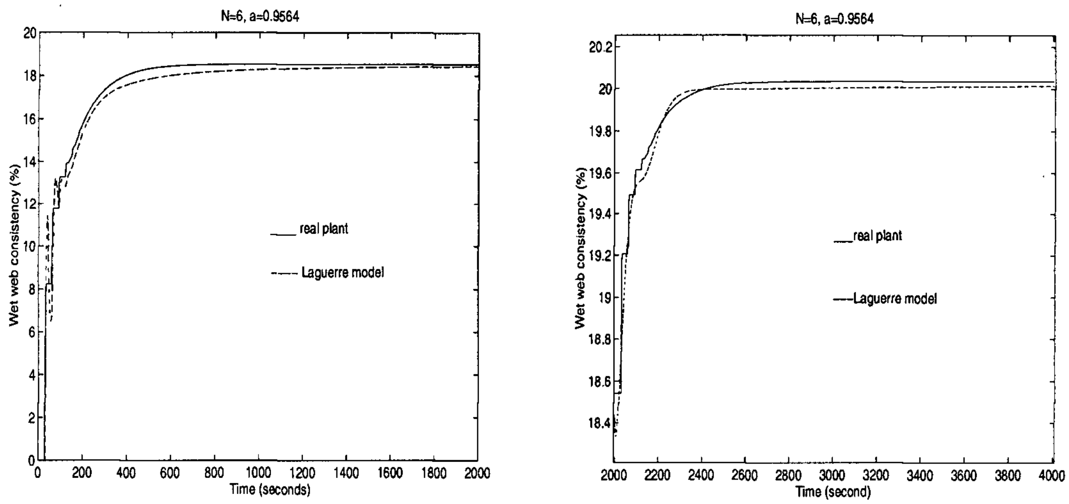

Figure 3.16: Identification result (N=6)

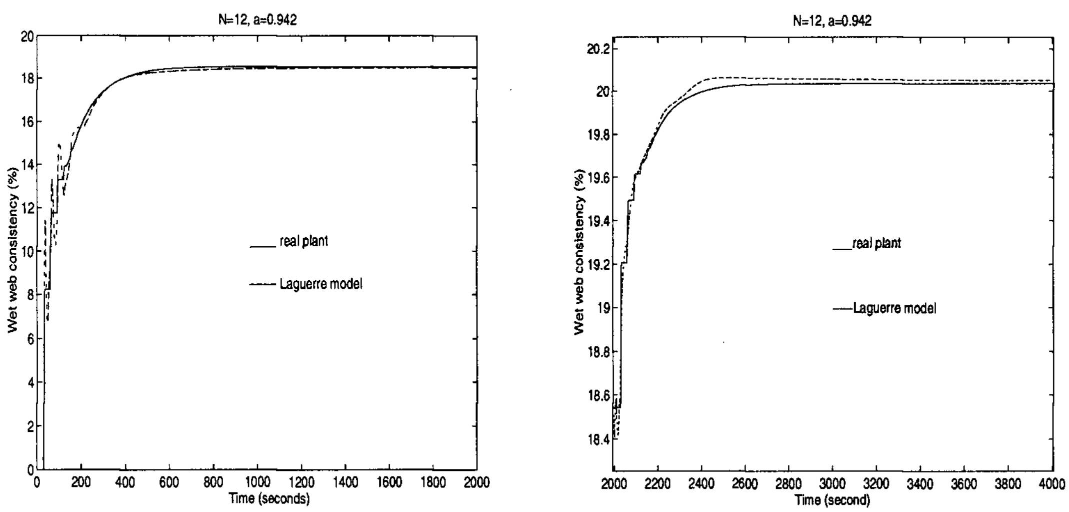

Figure 3.17: Identification result (N=12)

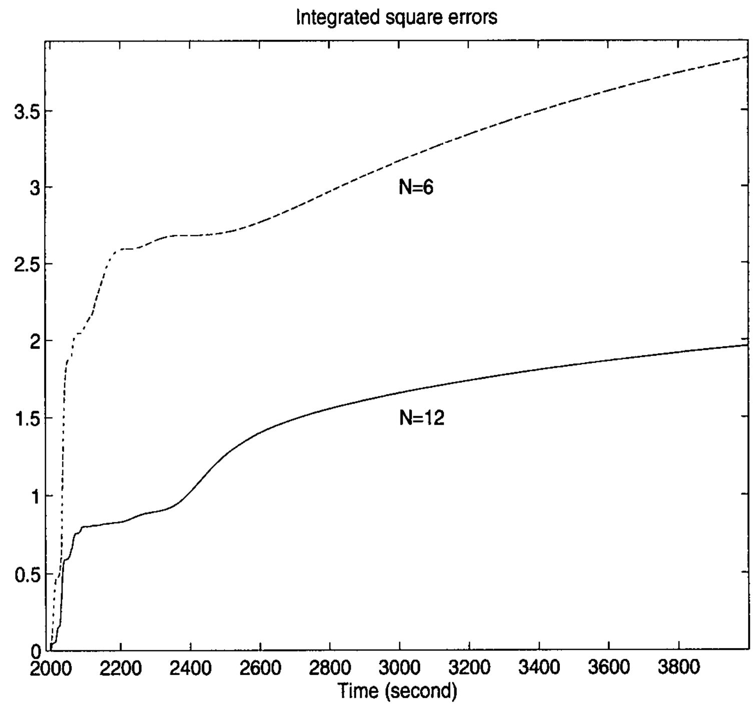

Figure 3.18: Comparison of the integrated square errors

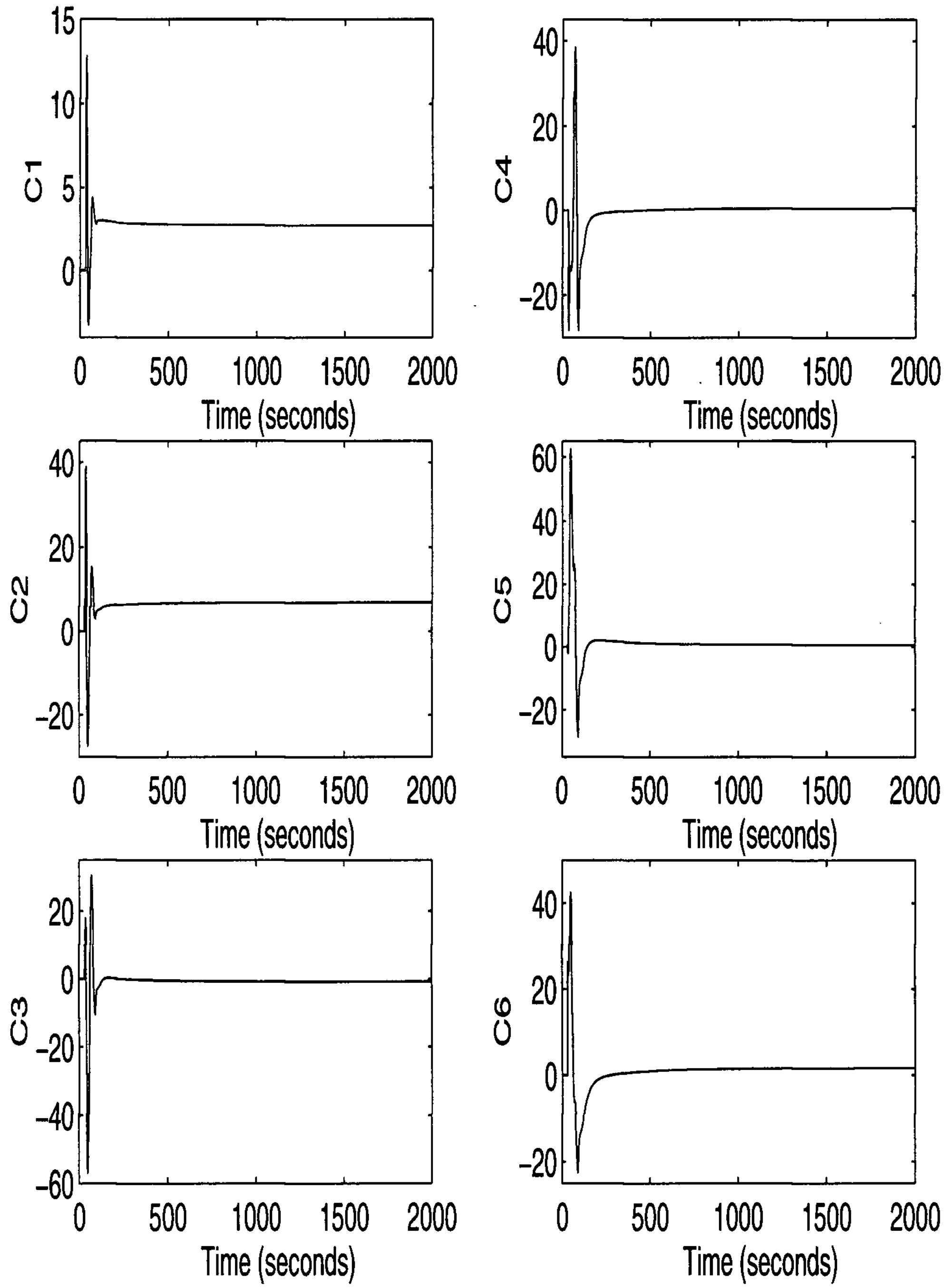

Figure 3.19: Estimated Laguerre filter coefficients (N=6)

Chapter 4

Control Design

In this chapter, a Laguerre model in the state space form is used to design an adaptive generalized predictive controller (GPC) for the white water recycle system. The robustness of this control scheme is discussed along with a summary of the choice of the control system design parameters. Finally, it is concluded with simulation results.

4.1 Background

With inter-related recycle loops, varying time delays and a wide range of uncertainties in the process, the white water system exhibits complicated dynamics. A controller for the white water recycle system must be able to handle unmeasurable disturbance, measurement noise, process time delays, as well as interactions from inside and outside the process etc.

It is well known that adaptive controllers can effectively adjust their control parameters to adapt changes in process dynamics and disturbance chracteristics. Adaptive control has evolved to a mature level. Considerable success has been achieved in this field in the past decades. Adaptive techniques are being used more and more in industrial control systems. Usually the design procedure involves three steps: model selection, parameter estimation and controller design. It has been proved that generalized predictive control (GPC) is a powerful control algorithm for adaptive control applications. GPC can be used to control a plant with little prior knowledge, variable dead-time and variable parameters provided that the input and output data are sufficiently rich for reasonable system identification. A standard version of the GPC using a recursive solution of the Diophantine equation for a linear CARIMA model was best summarized by Clarke, et. al. (1987) [29]. Since then, generalized predictive control and its modified forms are widely used with different model structures [21, 22, 30, 31]. From a modeling point of view, generalized predictive control schemes could be based on a structured model, e.g. ARMAX or CARIMA model, and an unstructured model, e.g. an impulse response model or an orthomormal series model. In the next section, a generalized predictive control algorithm based on a Laguerre model is derived for the control of paper machine white water recycle system. For adaptive control purpose, the Laguerre coefficients are estimated on-line using recursive least-squares(RLS) estimation method.

4.2 Control Algorithm

4.2.1 The Predictive Control Law

A discrete-time state space representation of the Laguerre-filters-based model can be written in the form

$$\boldsymbol{l}(t+1) = A\boldsymbol{l}(t) + \boldsymbol{b}u(t) \tag{4.52}$$

$$y(t) = \boldsymbol{c}^T\boldsymbol{l}(t) \tag{4.53}$$

Consider a j-step ahead predictor-corrector model, the future output has the form

$$\hat{y}(t+j) = c^T\boldsymbol{l}(t+j) + (y(t) - c^T\boldsymbol{l}(t)) \tag{4.54}$$

The first part in the right hand side of equation (4.54) is the system ouput at time$(t+j)$ determined by the model, while the second part is the correction for modelling errors or disturbances on the output of the process. Obviously, if there is no plant-model mismatch, the second part is equal to zero. Thus, this j-step predictor is in fact an observer.

Suppose $y_r(t+j)$(for $j = 1, 2, ...$) is a reference trajectory. In most cases, it is a constant with a value equal to the current setpoint y_{sp}. In order to achieve a smooth transition from current output $y(t)$ to a new setpoint, a reference trajectory with a simple first-order lag model is used as follows:

$$y_r(t) = y(t) \tag{4.55}$$

$$y_r(t+j) \quad = \quad \alpha y_r(t+j-1) + (1-\alpha)y_{sp} \tag{4.56}$$

where $\alpha (0 < \alpha < 1)$ is a coefficient for tuning the output convergence speed. The greater the coefficient, the slower the transition. Then the objective of the predictive control law is to drive plant outputs $y(t+j)$ to the reference trajectory $y_r(t+j)$ according to certain performance criteria. The choice of the criterion function is of paramount importance for the determination of the predictive control law. The standard generalized predictive control law is based on the following criterion function:

$$J = \sum_{j=H_m}^{H_p} [\hat{y}(t+j) - y_r(t+j)]^2 + \sum_{j=1}^{H_c} \beta[\triangle u(t+j-1)]^2 \tag{4.57}$$

where

H_p is the prediction horizon,

H_m is the minimum-cost horizon,

H_c is the control horizon,

β is the control-weighting factor ($\beta \geq 0$),

$\triangle$ is the differencing operator ($\triangle = 1 - q^{-1}$).

Now two conflicting objectives come up: the minimization of the tracking error and the minimization of the control increments. β is introduced to achieve a trade-off between these objectives. It is assumed that after the control horizon, further control increments are zero.

The resulting controller must be able to drive the plant outputs to a desired trajectory. Recalling the state space equations and recursively using equation 4.52

$$\begin{aligned} \boldsymbol{l}(t+1) &= A\boldsymbol{l}(t) + \boldsymbol{b}u(t) \\ \boldsymbol{l}(t+2) &= A\boldsymbol{l}(t+1) + \boldsymbol{b}u(t+1) \\ &\vdots \\ \boldsymbol{l}(t+j) &= A\boldsymbol{l}(t+j-1) + \boldsymbol{b}u(t+j-1) \end{aligned} \tag{4.58}$$

then $\boldsymbol{l}(t+j)$ can be obtained as

$$\boldsymbol{l}(t+j) = A^j\boldsymbol{l}(t) + A^{j-1}\,\boldsymbol{b}u(t) + A^{j-2}\,\boldsymbol{b}u(t+1) + \cdots + \boldsymbol{b}u(t+j-1) \tag{4.59}$$

Therefore, the future output is

$$\begin{aligned}\hat{y}(t+j) = \quad & \boldsymbol{c}^T[A^j\boldsymbol{l}(t) + A^{j-1}\ \boldsymbol{b}u(t) + A^{j-2}\ \boldsymbol{b}u(t+1) \\ & + \cdots +\ \boldsymbol{b}u(t+j-1)] + (y(t) - \boldsymbol{c}^T\boldsymbol{l}(t))\end{aligned} \tag{4.60}$$

It contains three parts: one is related to the current states, one is the current measured output, and the rest depends on future control actions. The first two parts depend on past controls which are known at time t, and $f(t+j)$ is used to represent them.

$$f(t+j) = \ \boldsymbol{c}^T[A^j - I]\boldsymbol{l}(t) + y(t) \tag{4.61}$$

To simplify the derivation below without loss of generality, the minimum-cost horizon H_m is set to 1, and the prediction horizon H_p to a reasonable larger number n. Then the predicted output can be written in a matrix form:

$$\hat{\boldsymbol{y}} = G\ \boldsymbol{u} +\ \boldsymbol{f} \tag{4.62}$$

where $\hat{\boldsymbol{y}}$, $\boldsymbol{f}$ and $\boldsymbol{u}$ are all $(n \times 1)$ vectors.

$$\hat{\boldsymbol{y}} = [\hat{y}(t+1), \hat{y}(t+2), ..., \hat{y}(t+n)]^T;$$
$$\boldsymbol{u} = [u(t), u(t+1), ..., u(t+n-1)]^T;$$
$$\boldsymbol{f} = [f(t+1), f(t+2), ..., f(t+n)]^T;$$

The matrix G is lower-triangular of dimention $(n \times n)$:

$$G = \begin{bmatrix} g_0 & 0 & \cdots & 0 \\ g_1 & g_0 & \cdots & 0 \\ \vdots & \ddots & \ddots & \vdots \\ g_{n-1} & g_{n-2} & \cdots & g_0 \end{bmatrix} \tag{4.63}$$

where the elements $g_j(j = 0, 1, ..., n-1)$ are the system impulse-response coefficients which are given by

$$g_j = \boldsymbol{c}^T A^j \boldsymbol{b}$$

In the criterion function in eqation (4.57), the controller increments are weighted instead of the controller outputs. Therefore to derive the control law by minimizing the criterion function, the predicted output representation should contain control signal increment term other than control signal itself. Define

$$\boldsymbol{u_1} = [u(t-1), u(t-1), ..., u(t-1)]^T$$

then equation (4.62) can be rewritten in the form

$$\hat{\boldsymbol{y}} = G(\boldsymbol{u} - \boldsymbol{u_1}) + G\boldsymbol{u_1} + \boldsymbol{f} \tag{4.64}$$

the j-th element of vector $(\boldsymbol{u} - \boldsymbol{u_1})$ is

$$\begin{aligned} u(t+j) - u(t-1) &= u(t+j) - u(t+j-1) + ... + u(t) - u(t-1) \\ &= \triangle u(t+j) + \triangle u(t+j-1) + ... + \triangle u(t) \end{aligned} \tag{4.65}$$

therefore, the vector can be written in the form

$$(\boldsymbol{u} - \boldsymbol{u_1}) = I_1 \triangle \boldsymbol{u} \tag{4.66}$$

where, $\triangle \boldsymbol{u}$ is the control increment vector

$$\triangle \boldsymbol{u} = [\triangle u(t), \triangle u(t+1), ..., \triangle u(t+n-1)]^T$$

and I_1 is a unit lower-angular matrix of dimension $(n \times n)$

$$I_1 = \begin{bmatrix} 1 & 0 & \cdots & 0 \\ 1 & 1 & \cdots & 0 \\ \vdots & \ddots & \ddots & \vdots \\ 1 & 1 & \cdots & 1 \end{bmatrix}$$

Furthermore, the predicted output can be written in a control increment vector form

$$\hat{\boldsymbol{y}} = H\triangle \boldsymbol{u} + G\boldsymbol{u_1} + \boldsymbol{f} \tag{4.67}$$

where

$$H = GI_1$$

Obviously, H is a $n \times n$ lower-triangular matrix

$$H = \begin{bmatrix} h_0 & 0 & \cdots & 0 \\ h_1 & h_0 & \cdots & 0 \\ \vdots & \ddots & \ddots & \vdots \\ h_{n-1} & h_{n-2} & \cdots & h_0 \end{bmatrix} \tag{4.68}$$

the elements $h_j (j = 0, 1, ..., n-1)$ are system step-response coefficients and

$$\begin{cases} h_j = g_j, & j = 0 \\ h_j = g_j + h_{j-1}, & j = 1, 2, ..., n-1 \end{cases} \tag{4.69}$$

Then, the criterion function (4.57) can be written in a matrix form

$$J = (\hat{\boldsymbol{y}} - \boldsymbol{y_r})^T (\hat{\boldsymbol{y}} - \boldsymbol{y_r}) + \beta (\triangle \boldsymbol{u})^T \triangle \boldsymbol{u} \tag{4.70}$$

Substituting equation 4.67 into above criterion function, it becomes

$$J = (H \triangle \boldsymbol{u} + G \boldsymbol{u_1} + \ \boldsymbol{f} - \boldsymbol{y_r})^T (H \triangle \boldsymbol{u} + G \boldsymbol{u_1} + \ \boldsymbol{f} - \boldsymbol{y_r}) + \beta (\triangle \boldsymbol{u})^T \triangle \boldsymbol{u} \tag{4.71}$$

To derive the control law,

$$\frac{\partial J}{\partial \triangle \boldsymbol{u}} = 2H^T (H \triangle \boldsymbol{u} + G \boldsymbol{u_1} + \ \boldsymbol{f} - \boldsymbol{y_r}) + 2\beta \triangle \boldsymbol{u} = 0 \tag{4.72}$$

Finally, the control increment vector is obtained as follows (a similar result is shown in [33](1991)):

$$\triangle \boldsymbol{u} = (\beta I + H^T H)^{-1} H^T (\boldsymbol{y_r} - G \boldsymbol{u_1} - \ \boldsymbol{f}) \tag{4.73}$$

Note that only the first element of $\triangle \boldsymbol{u}$ is used as the current control increment. All other elements are not used and need not calculated. Then the control law can be written in a simple form

$$u(t) = u(t-1) + \boldsymbol{h}^T (\boldsymbol{y_r} - \boldsymbol{g}) \tag{4.74}$$

where $\boldsymbol{h}^T$ is the first row of $(\beta I + H^T H)^{-1} H^T$ and $\boldsymbol{g}$ stands for $G\boldsymbol{u_1} + \ \boldsymbol{f}$ which is determined by past known control $u(t-1)$.

4.2.2 Robustness Analysis

In practice, mismatch between a real process and its model is always present. As mentioned in chapter 3, an infinite Laguerre series can be used to exactly represent a stable system. But it is more realistic to use a truncated Laguerre series for process modeling. In this case, the plant/model mismatch is caused by the truncation error. Therefore it is important to investigate the influence of modeling errors on system performance. A closed-loop system is robust if the system response maintains certain properties even though the ture process is different from its model.

Assume the plant is modelled by a n-th order trancated Laguerre function,

$$\boldsymbol{l}(t+1) = A\boldsymbol{l}(t) + \boldsymbol{b}u(t) \tag{4.75}$$

$$y(t) = \boldsymbol{c}^T\boldsymbol{l}(t) \tag{4.76}$$

the real system is represented by the following Laguerre function:

$$\begin{bmatrix} \boldsymbol{l}(t+1) \\ \tilde{\boldsymbol{l}}(t+1) \end{bmatrix} = \begin{bmatrix} A & 0 \\ \tilde{A}_1 & \tilde{A}_2 \end{bmatrix} \begin{bmatrix} \boldsymbol{l}(t) \\ \tilde{\boldsymbol{l}}(t) \end{bmatrix} + \begin{bmatrix} \boldsymbol{b} \\ \tilde{\boldsymbol{b}} \end{bmatrix} u(t) \tag{4.77}$$

$$y(t) = \begin{bmatrix} \boldsymbol{c}^T & \tilde{\boldsymbol{c}}^T \end{bmatrix} \begin{bmatrix} \boldsymbol{l}(t) \\ \tilde{\boldsymbol{l}}(t) \end{bmatrix} \tag{4.78}$$

where, the order of state vector $\tilde{\boldsymbol{l}}(t)$ is large enough (tend to ∞), it is assumed that this model can be used to accurately represent the real plant in some sense.

Recall the control increment vector equation (4.73):

$$\triangle\boldsymbol{u} = (\beta I + H^T H)^{-1} H^T(\boldsymbol{y_r} - G\boldsymbol{u_1} - \boldsymbol{f}) \tag{4.79}$$

For a reasonable small control horizon ($H_c << H_p$), the control increments are zero for $t > H_c$. The calculation for the control $\triangle\boldsymbol{u}$ can be significantly decreased. Only the first H_c columns of H are required to calculate the corresponding control law. The matrix involved in the inversion is a reduced dimension ($H_c \times H_c$). For simplification, a value of H_c of 1 is considered here.

Generally speaking, a one-step control horizon gives acceptable control for typical industrial plants. Then the control has the following scalar form:

$$\triangle u = (\beta + H_1^T H_1)^{-1} H_1^T(\boldsymbol{y_r} - G\boldsymbol{u_1} - \boldsymbol{f}) \tag{4.80}$$

where H_1 is the first column of H, that is

$$H_1^T = [h_0, h_1, ..., h_{n-1}] \tag{4.81}$$

$$h_i = \sum_{j=0}^{i-1} \boldsymbol{c}^T A^j \boldsymbol{b} \tag{4.82}$$

and

$$G\boldsymbol{u_1} = H_1 u(t-1)$$

From equation (4.61), $f(t+j)$ can be derived as:

$$\begin{aligned} f(t+j) &= \boldsymbol{c}^T A^j \boldsymbol{l}(t) - \boldsymbol{c}^T \boldsymbol{l}(t) + y(t) \\ &= \boldsymbol{c}^T A^j \boldsymbol{l}(t) - (\hat{y}(t) - y(t)) \end{aligned} \tag{4.83}$$

Furthermore,

$$H_1^T \boldsymbol{f} = \sum_{j=0}^{n-1} h_j \boldsymbol{c}^T A^{j+1} \boldsymbol{l}(t) - \sum_{j=0}^{n-1} h_j(\hat{y}(t) - y(t)) \tag{4.84}$$

Suppose the output setpoint is considered as the reference trajectory, thus the control law derived from a truncated Laguerre model is

$$u(t) = m\{w(y_{sp} + \hat{y}(t) - y(t)) - \boldsymbol{s}^T \boldsymbol{l}(t) + \beta u(t-1)\} \tag{4.85}$$

where

$$m = (\beta + H_1^T H_1)^{-1} \tag{4.86}$$

$$\boldsymbol{s}^T = \sum_{j=0}^{n-1} h_j \boldsymbol{c}^T A^{j+1} \tag{4.87}$$

$$w = \sum_{j=0}^{n-1} h_j \tag{4.88}$$

then, with the control law designed based on a truncated Laguerre model, the closed-loop system of the real plant is given by

$$\begin{aligned} \begin{bmatrix} \boldsymbol{l}(t+1) \\ \tilde{\boldsymbol{l}}(t+1) \end{bmatrix} &= \begin{bmatrix} A - m\ \boldsymbol{b}\ \boldsymbol{s}^T & 0 \\ \tilde{A}_1 - m\ \tilde{\boldsymbol{b}}\ \boldsymbol{s}^T & \tilde{A}_2 \end{bmatrix} \begin{bmatrix} \boldsymbol{l}(t) \\ \tilde{\boldsymbol{l}}(t) \end{bmatrix} \\ &+ \begin{bmatrix} \boldsymbol{b} \\ \tilde{\boldsymbol{b}} \end{bmatrix} mw(y_{sp} + \hat{y}(t) - y(t)) + \begin{bmatrix} \boldsymbol{b} \\ \tilde{\boldsymbol{b}} \end{bmatrix} m\beta u(t-1) \end{aligned} \tag{4.89}$$

The system state response is affected by three parts: state variable values at time t ($\left[\boldsymbol{l}(t), \tilde{\boldsymbol{l}}(t)\right]^T$), modelling error at time t (difference between model output and system output $\hat{y}(t) - y(t)$) and the input signal at previous step $u(t-1)$. To see the regulator behaviour and to simplify the derivation, assume that $y_{sp} = 0$ and $\beta = 0$, and define the state vector:

$$\boldsymbol{L}(t) = \left[\ \boldsymbol{l}^T\ \tilde{\boldsymbol{l}}^T \right]^T \tag{4.90}$$

Then, the closed-loop system can be written in a matrix form:

$$\boldsymbol{L}(t+1) = \left[\ \boldsymbol{A} + Bmw(\hat{\boldsymbol{C}}^T - \ \boldsymbol{C}^T)\right]\ \boldsymbol{L}(t) \tag{4.91}$$

where

$$\boldsymbol{A} = \begin{bmatrix} A - m\ \boldsymbol{b}\ \boldsymbol{s}^T & 0 \\ \tilde{A}_1 - m\ \tilde{\boldsymbol{b}}\ \boldsymbol{s}^T & \tilde{A}_2 \end{bmatrix} \tag{4.92}$$

$$B = \left[\boldsymbol{b}\ \tilde{\boldsymbol{b}}\right]^T \tag{4.93}$$

$$\hat{\boldsymbol{C}}^T = \left[\hat{\boldsymbol{c}}^T \boldsymbol{0}^T\right] \tag{4.94}$$

$$\boldsymbol{C}^T = \left[\hat{\boldsymbol{c}}^T\ \tilde{\boldsymbol{c}}^T\right] \tag{4.95}$$

$\hat{\boldsymbol{c}}^T$ contains the estimated coefficients of the truncated Laguerre model. For a stable system, the state variables must converge to certain values in some sense. Therefore

$$\|\ \boldsymbol{A}\| + \|B\||m|w\||\hat{\boldsymbol{C}}^T - \ \boldsymbol{C}^T\| < 1 \tag{4.96}$$

must be satisfied. In other words, the coefficient difference between the model and the real system should be kept as small as possible to achieve good robustness. That is

$$||\hat{\boldsymbol{C}}^T - \boldsymbol{C}^T|| < \frac{1 - ||\ \boldsymbol{A}||}{m|w|||B||} \tag{4.97}$$

It shows that the GPC robustness can be improved by changing related design parameters.

4.2.3 Choice of Design Parameters

How to select design parameters, such as prediction horizon, minimum-cost horizon, control horizon and control weighting factor, always has a significant impact on closed-loop system performance. Certain general rules for the selection of these parameters were discussed by Clarke et al. (1987) [29]. These studies are widely accepted as rules of thumb for the GPC design. Here the methods are summarized as follows:

- **Minimum-cost horizon H_m:** It is effective to set the minimum-cost horizon larger than the dead-time of the process, because there is some time delay for the outputs to respond to the corresponding control action. There is no need to calculate the outputs that cannot be affected by the first control signal $u(t)$. In the cases when the dead-time is unknown or variable, the minimum-cost horizon can be set to 1 to maintain stability and encompass all possible values of dead-time.

- **Prediction horizon H_p:** For an open-loop stable system, it is better to use a larger value for the prediction horizon, normally close to the rise time of the process. In this case, the major part of the transient response is involved. Increasing H_p results in a smoother controller output.

- **Control horizon H_c:** The control horizon is an important design parameter. Generally, a value of 1 gives acceptable control for typical industrial plant models. But for a complex system, the control action might have significant change at the next sample, it is necessary to take more future control sequences into account for the calculation at each sample. A short control horizon would not allow for enough degrees of freedom in the derivation of the current control action. In general, increasing the control horizon makes the control and the corresponding output response more active.

- **Control-weighting factor β:** The control-weighting factor is introduced to make a trade-off between two conflicting objectives: the minimization of the tracking error and the minimization of the controller output increment. A greater weighting factor means that the controller output is more important in the criterion function. The control law based on this criterion function is less active and the process output becomes less important resulting in a sluggish process response. Although the effect of the weighting factor on the closed-loop system is clearly expressed in the criterion function, it is hard to choose a value of β to achieve desired system behaviour. It is usually determined by simulations in combination with trial-and-error method.

4.3 Simulations and Discussions

4.3.1 Generalized Predictive Control Behaviour

This section studies Laguerre model based GPC control performance through simulation results. The simulations are carried out for different prediction horizon(H_p) and minimum-cost horizon (H_m). The effect of control horizon (H_c) is also discussed in those simulations.

The white water recycle system is modelled by a 12th order Laguerre function with filter pole $a = 0.942$ and Laguerre coefficients

$$\begin{aligned} \boldsymbol{c}^T = [&1.8951, 6.3968, 2.4267, -1.1200, 1.0462, 2.0494, \\ &-2.7392, 4.9367, -4.2792, 3.7254, -2.0496, 1.2049] \end{aligned}$$

These coefficients are the estimated results in chapter 3. Based on this model, the GPC control law derived in the previous section is used to control the plant. Closed-loop simulations with the structure as shown in figure 4.20 are carried out for different design parameters referred to in the figures. The simulation program is attached in the appendix (program 2).

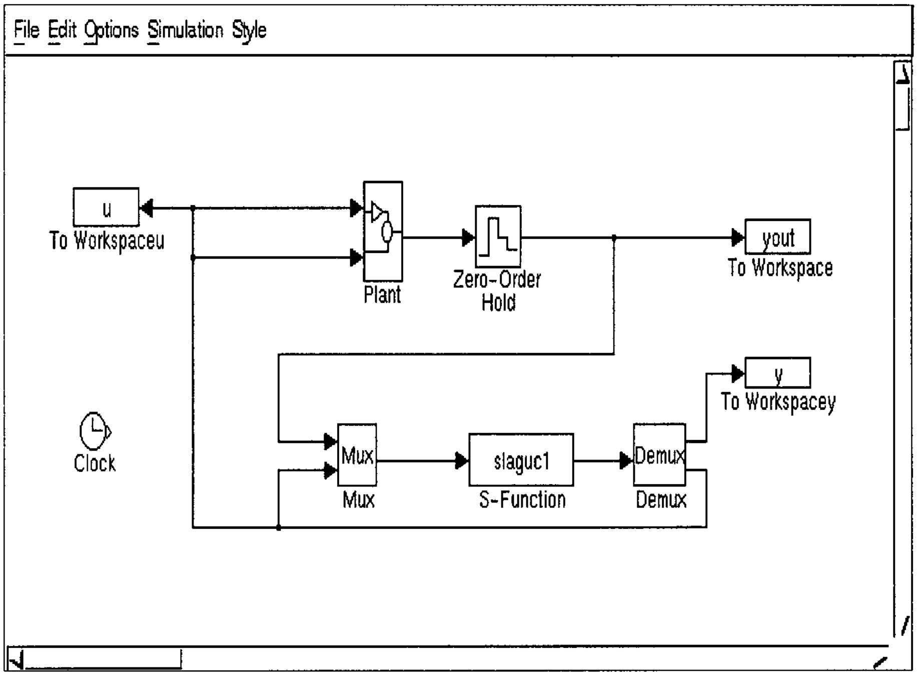

Figure 4.20: Laguerre model based GPC simulation diagram

First, based on the methods described in the previous section and combining with trial and error, a set of typical design paramters are chosen to be $H_p = 100$, $H_m = 60$, $H_c = 1$ and $\beta = 0.1$. The step response of the white water recycle system in chapter 2 shows that 100 seconds covered most of the transient message of the process. The system dead-time is around 30 seconds. To reasonably decrease calculations and at the same time to take major transient response into account for the calculation of the corresponding control actions, the minimum-cost horizon is set to 60. For an open-loop stable plant, an one-step control horizon can be used to give reasonable performance. Increasing the control horizon makes the control and corresponding output response more active. Because the white water recycle system is a stable process, here a small control weighting factor ($\beta = 0.1$) is used for the purpose of keeping the control action active. The simulation results with sampling interval 1 second are shown in figure 4.21. Effective servo performance is achieved. The predictive controller can take early action to overcome process dead-time when the set point changes is known a priori.

For the prediction horizon, simulations for three different values ($H_p = 70, 80$ and 90) are carried out. While other parameters are seperately set to $H_m = 50$, $H_c = 1$ and $\beta = 0.1$. The prediction horizon and control horizon are closely related to the stability of the closed-loop system. The effect of H_p with $H_c = 1$ on the system performance are shown in figure 4.22. Obviously, when H_p increases, the closed-loop response is slower to set point changes and the resulting control action is more smooth and sluggish. The behaviour of the closed-loop system can also be influenced by H_c in a similar way to that when using H_p. In contrast, increasing H_c makes the control and the corresponding output response more active.

For the minimum-cost horizon, similarly, simulations for three different values ($H_m = 50, 70$ and 80) are carried out. Other parameters are respectively set to $H_p = 100$, $H_c = 1$ and $\beta = 0.1$. For this process, increasing the minimum-cost horizon makes the closed-loop system respond more slowly to set point changes, and an increase of robustness can also be expected. But the choice for H_m is not very critical. For the purpose of decreasing the calculations, H_m should be chosen greater than system dead-time. The effect of H_m on the system performance are shown in figure 4.23.

4.3.2 Adaptive Generalized Predictive Control Behaviour

The white water recycle system and its environment are changing all the time. When the white water system is closed up, great amount of information, such as water quality, materials management and deposition control, will affect paper machine performance. These disturbances appear randomly, but they have strong impact on product properties. To insure that the paper machine is running effectively, a controller that can modify its behaviour in response to changes in the dynamics of the process and the character of the disturbances is required for the control of the white water recycle system. This is exactly the basic concept of what an adaptive controller is. Based on the updated estimates of the process parameters, the controller parameters are modified from the solution of a design problem. As derived in the previous chapters, in this thesis a straightforward combination of recursive least-squares estimation and generalized predictive control algorithm gives an adaptive control scheme for the white water recycle system. The generalized predictive control law in equation (4.74) is calculated based on estimated Laguerre coefficients. Figure 4.24 shows the behaviour of the Laguerre model based adaptive controller with design parameters: $H_p = 100$, $H_m = 60$, $H_c = 1$ and $\beta = 0.1$, and with load disturbance of amplitude 0.01 from time $t = 1000$. The other two figures show the behaviour of the same controller for the plant dynamics changes. In figure 4.25, the recycle path time delay changes from 72 seconds to 30 seconds at time $t = 850$. Figure 4.26 is the response with forward path time delay change from 30 seconds to 20 seconds at time $t = 850$. The simulation program is attached in Appendix (program 3). As shown in those figures, this control scheme can achieve excellent servo performance and load disturbance rejection without steady-state offset. These are the direct results of adaptive GPC algorithm.

4.4 Conclusions

It has been proven in the GPC literature that GPC is a robust algorithm for adaptive control applications. In the criterion function of GPC, the control increments are weighted instead of the control outputs. Therefore, in the steady state the control weighting factor β won't affect the criterion function and the controller output which is obtained by minimizing the criterion function. This results in a control scheme free of steady-state offset, robust to system parameter variation and dead-time variation. The use of the GPC algorithm in an adaptive fashion makes the resulting controller even more powerful for dealing with unstructured uncertainties. During the last two decades, many research works have been done in this area. Most of them are based on the usual parametric ARMAX transfer function model. Motivated by the idea for a robust adaptive control for the process with minimal a priori information, some researchers have studied the robustness and stability of adaptive GPC based on Laguerre series representation, as discussed in the previous sections. This research presented the first application of the Laguerre model based adaptive GPC for the control of the challenging recycle processes.

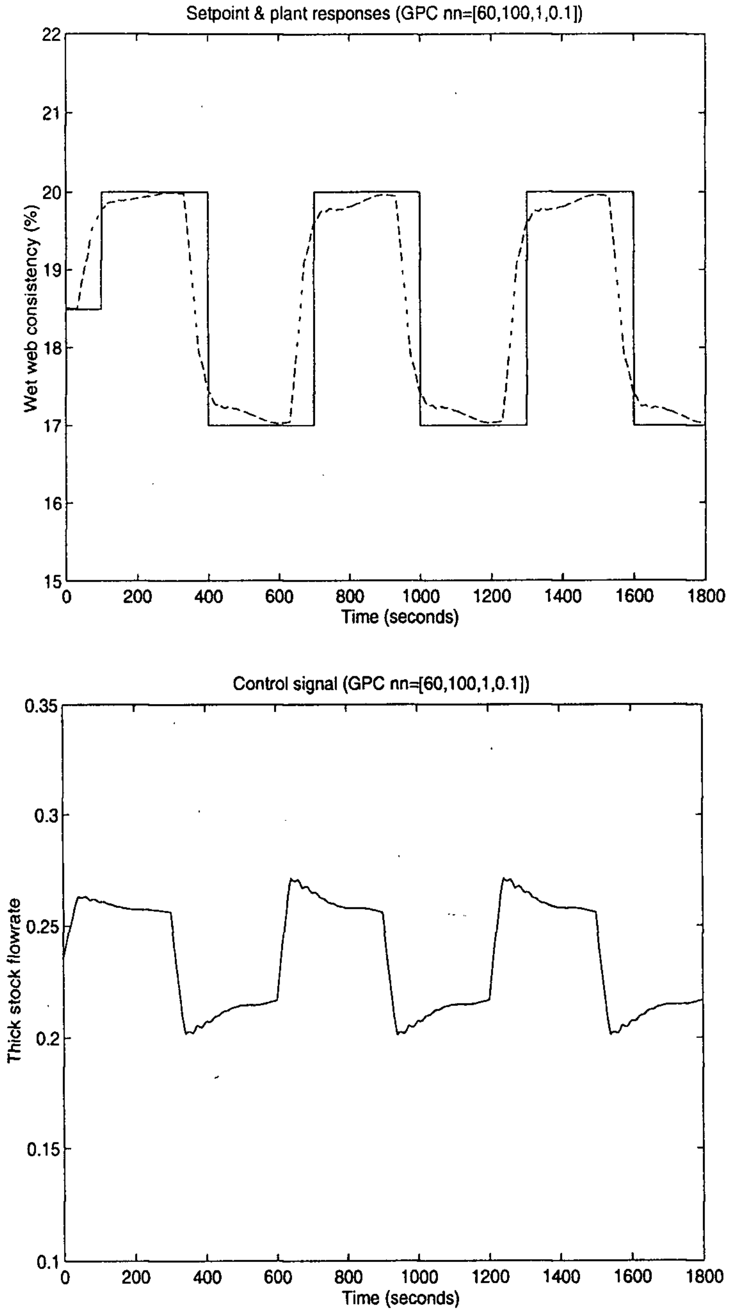

Figure 4.21: Laguerre model based GPC control response

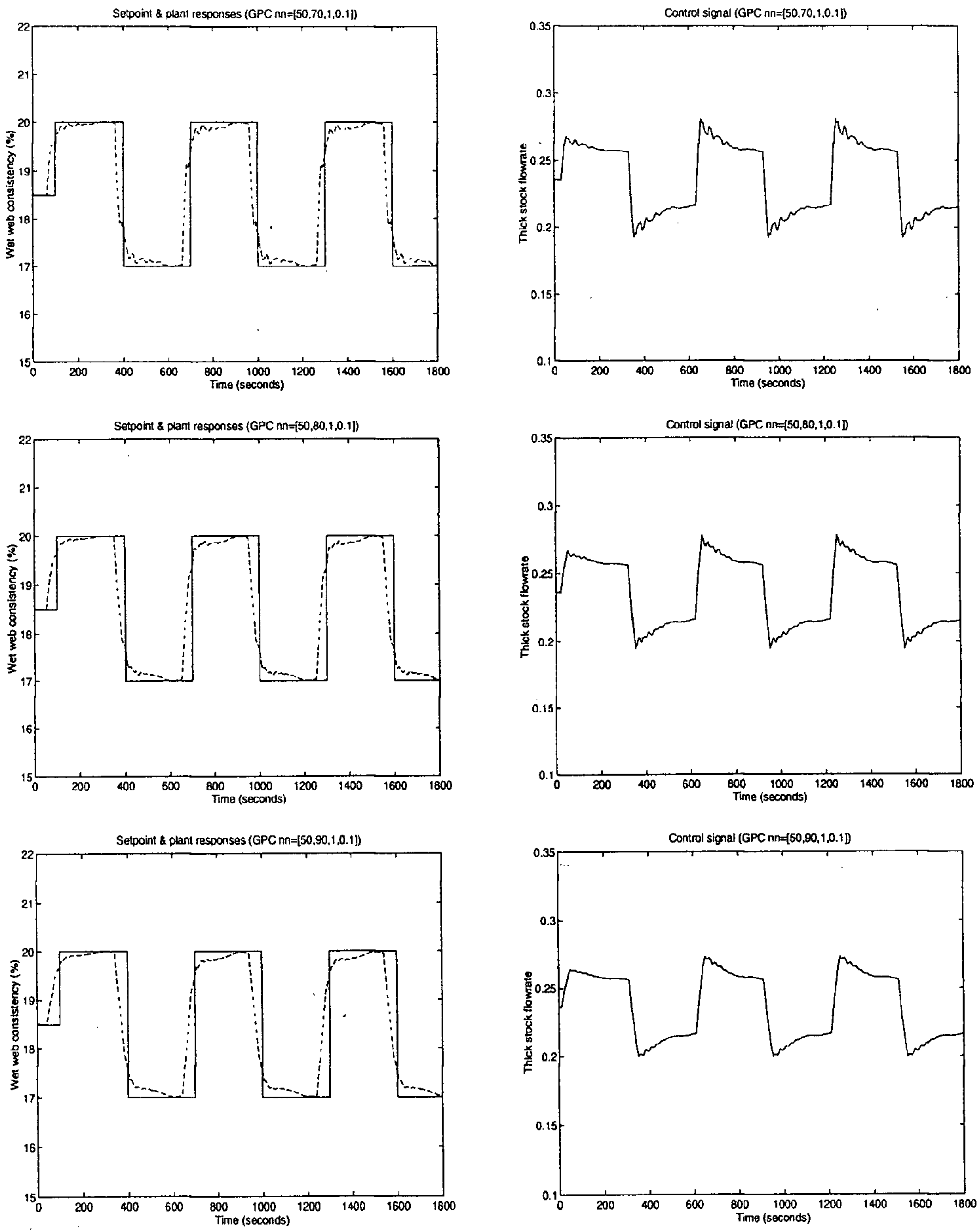

Figure 4.22: The effect of the prediction horizon on the closed-loop system response for Hp=70, 80 and 90.

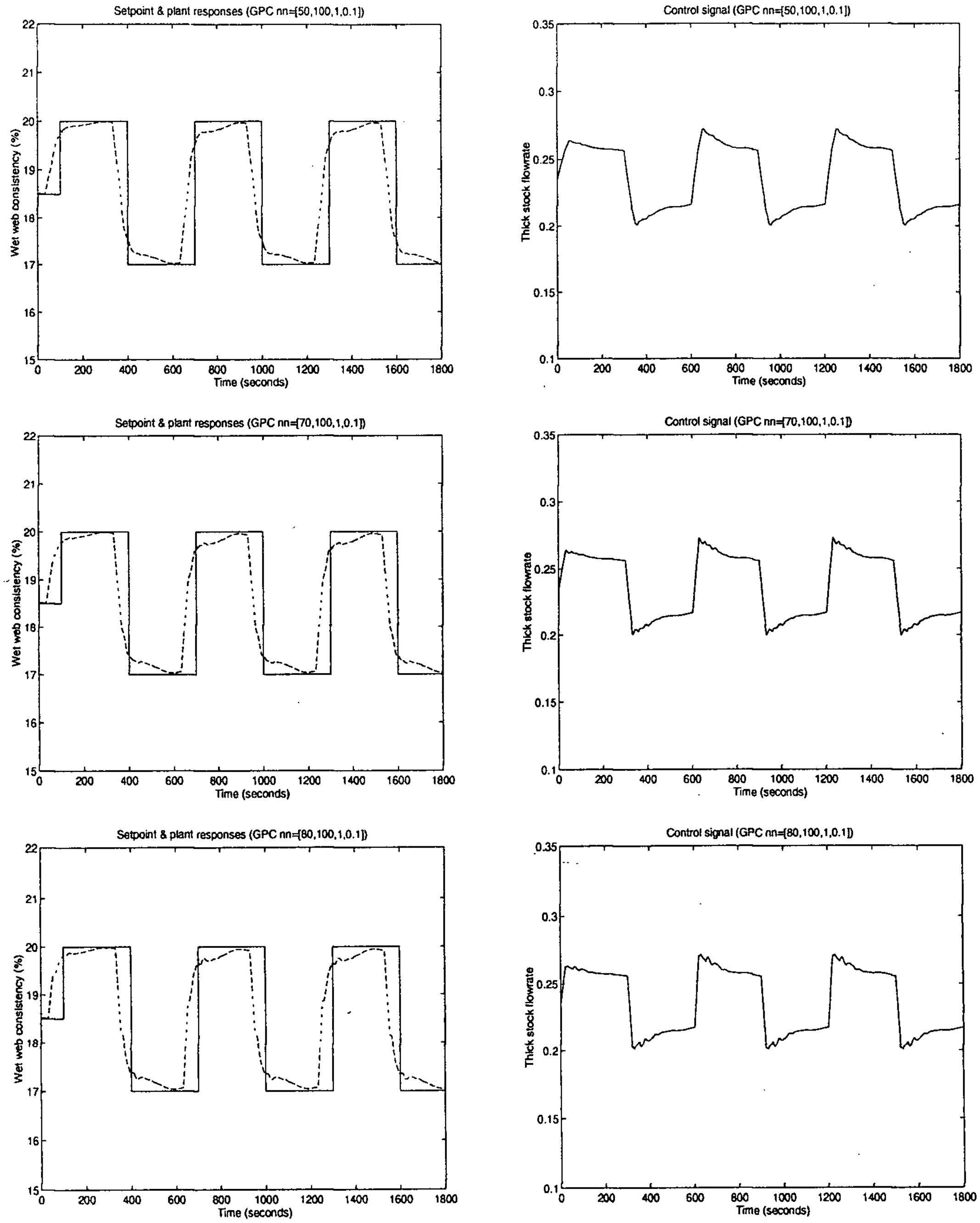

Figure 4.23: The effect of the minimum-cost horizon on the closed-loop system response for Hm=50, 70 and 80.

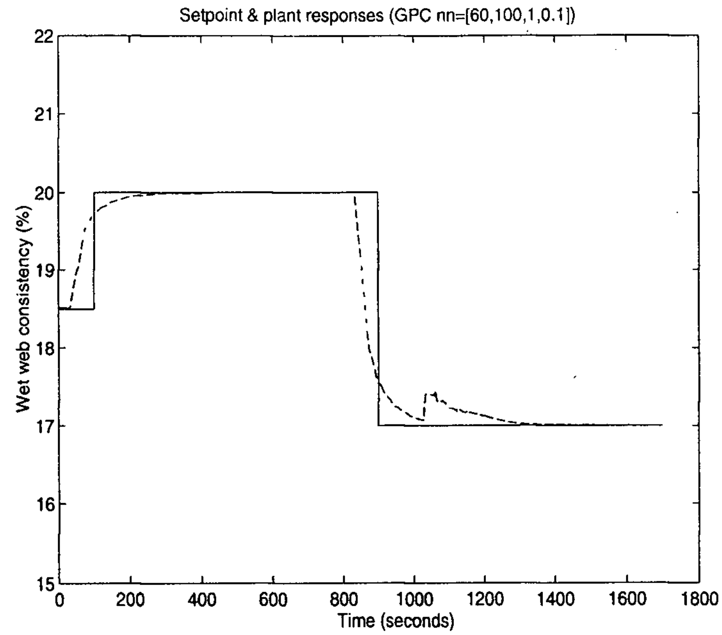

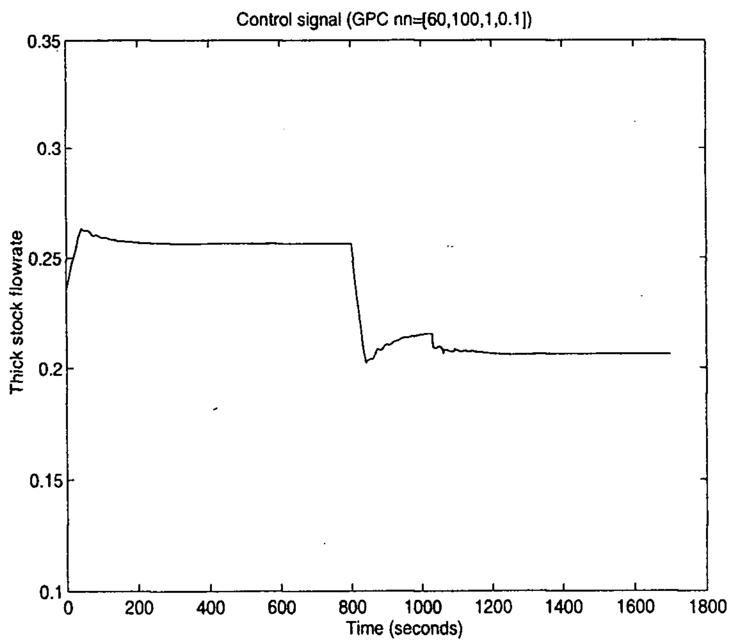

Figure 4.24: Adaptive GPC control responses with load disturbance at t=1000

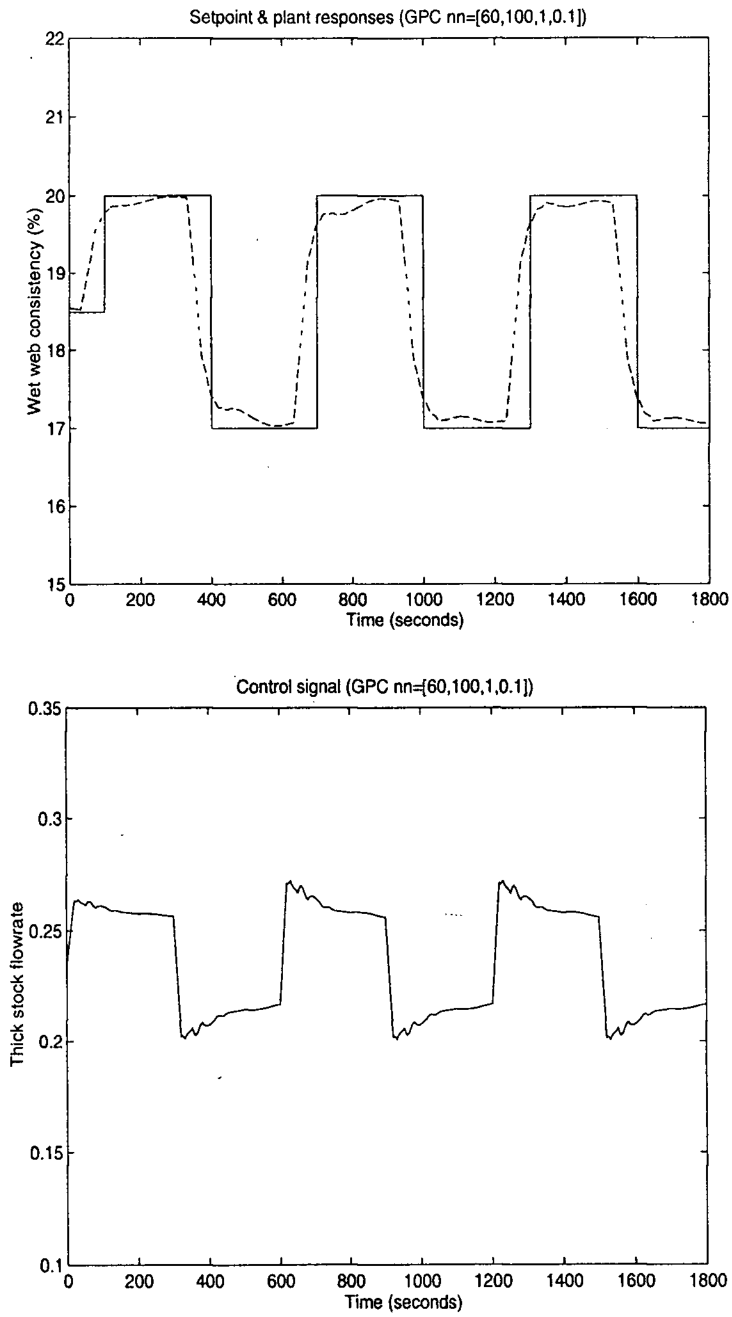

Figure 4.25: Adaptive GPC control responses with recycle time delay change at t=850

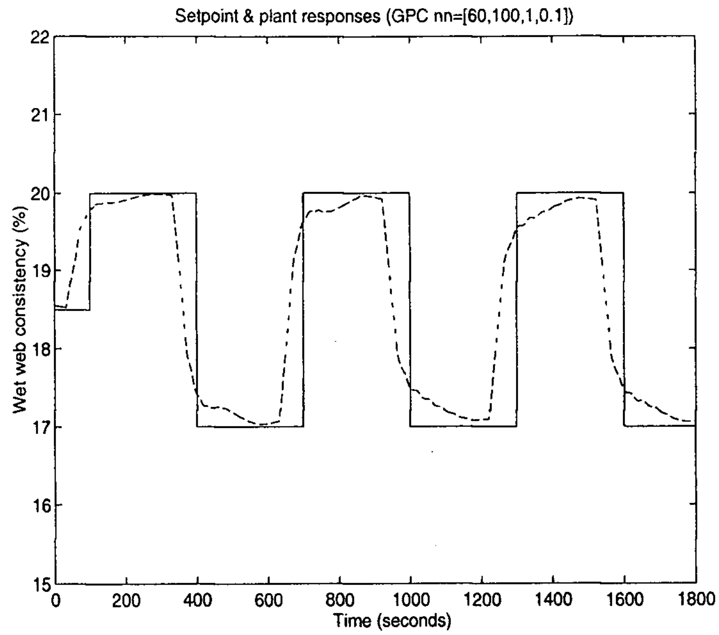

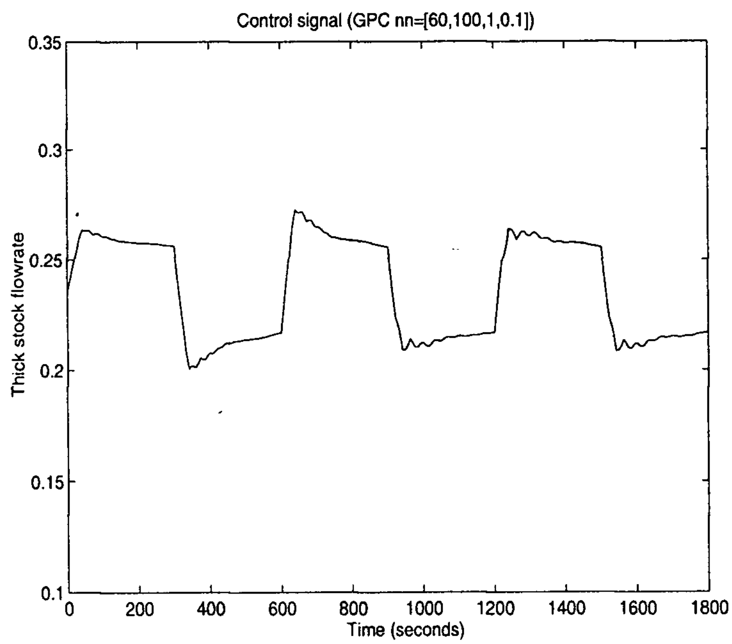

Figure 4.26: Adaptive GPC control responses with forward path time delay change at t=850

Chapter 5

Conclusions

5.1 Summary and Contributions

This thesis is focused on paper machine white water recycle dynamics and deals with the challenging problem of the processes with recycle loops. The open-loop system was analysed by exploring some intrinsic phenomena which are caused by the recycle streams. Motivated by its simplicity and strong features in modelling unstructured processes, the Laguerre series representation was used for on-line identification of the system dynamics. As a powerful control algorithm for adaptive control applications, a generalized predictive control based on a discrete-time state-space representation of the Laguerre model was used. Computer simulations were developed to examine control system performance. The major results and contributions of this thesis can be concluded as follows:

- With inter-related recycle flows from different stages of the paper machine, the paper machine white water system exhibits complex dynamics. Process analysis revealed some interesting and important phenomena that exist in the white water recycle system. Open-loop analysis demonstrates that the recycle process exhibits typical dynamics with transients caused by main flow and recycle flows respectively. The recycling increases both system time constant and steady-state gain. The increase in the steady-state gain is a direct result of the fibre reuse in the white water system. This is one of the immediate objectives of closing paper mill white water system. Each individual unit in the system affects different properties of the overall process dynamics. The units in the forward path have dominant effects on the overall system performance. And they also have strong impacts on the recycle flows, because the recycle flows pass through the forward path twice before they leave the plant. Mainly, the units in the recycle path only affect the dynamics of the recycle flows. These phenomena are the general rules for the recycle systems without a single exception. These results are quite useful for the study of any other recycle systems.

- In the white water system, different time delays exist in the forward path, recycle path and other units of the process. An accurate model is essential for improving the control of paper machine. The Laguerre series representation is extremely useful for the white water system modelling because of its simple ladder network form and strong features in identifying system uncertainty and time delays. And the Laguerre function coefficients can be easily identified by using least-squares estimation based on its convenient state space functions. For a fixed number of the Laguerre filters, there is an optimal Laguerre pole that minimizes the modelling error. Therefore searching for this optimal pole is a crucial issue as discussed in chapter 3. The simulation results showed that the Laguerre model provided a good plant/model match for the white water recycle system. These results support the use of this model for on-line identification and adaptive control.

- A controller for the white water recycle system must be able to handle unmeasurable disturbances, process time delays, interactions from inside and outside the plant etc. Adaptive controllers can effectively adjust their control parameters to adapt changes in process dynamics and disturbances. It has been proven that generalized predictive control (GPC) is a powerful control algorithm for adaptive control applicaitons. The proposed adaptive GPC scheme achieved effective control performance for this complicated nonlinear recycle system. As discussed in chapter 4, this control strategy is robust to the variation of the time delays. It also provides excellent servo performance and load disturbance rejection.

5.2 Suggestions for Future Work

This thesis studied process dynamics, modelling and control of the white water recycle system. The results of this work could set the stage for the future work in this area. The system considered in this thesis is a deterministic model without system noise. Therefore, further research focused on disturbance investigation and regulator behaviour should be carried out. And further analysis of robustness and stability is necessary to find out the relationship between the control design parameters and the system performance. Furthermore, a frequency domain analysis is suggested to reveal system frequency performance.

Bibliography

[1] E.R.Gilliland, L.A.Gould and T.J. Boyle. *Joint Automatic Control Conference.* 1964; p 140.

[2] X.E.Verykios and W.L. Luyben. *Steady state sensitivity and dynamics of a reactor/distillation column system with recycle.* ISA Trans. 1978,17(2),31-41.

[3] W.L. Luyben and P.S. Buckley. *A Proportional-Only Level Controller Without Steadystate Offset.* Inst. Tech. 1977,24,65.

[4] M.M.Denn and R. Lavie. *Dynamics of plants with recycle.* Chem. Eng. J. 1982,24,55-59.

[5] N. Kapoor, T.E.Marlin and T.J.McAvoy. *Effect of recycle structure on distillation tower time constants.* AIChE J. 1986,32(3),411-418.

[6] W.L.Luyben. *The concept of eigenstructure in process control.* Ind. Eng. Chem. Res. 1988,27, 206-208.

[7] W.L.Luyben. *Dynamics and control of recycle systems. 1. Simple open-loop and closed-loop systems.* Ind.Eng.Chem.Res. 1993a,32(3),466-475.

[8] W.L.Luyben. *Dynamics and control of recycle systems. 2. Comparison of alternative process designs.* Ind.Eng.Chem.Res. 1993b,32(3),476-485.

[9] W.L.Luyben. *Dynamics and control of recycle systems. 3. Alternative process designs in a ternary system.* Ind.Eng.Chem.Res. 1993c, 32(6),1142-1153.

[10] P.W.Belanger and W.L. Luyben. *Inventory control in processes with recycle.* Ind. Eng. Chem. Res. 1997,36, 706-716.

[11] B.Panchapakesan. *White water reuse and savealls.* Pulp and Paper Manufacture, volume 6 173-185.

[12] N.Ryti and H. Paulapuro. *Stock and white water systems.* Pulp and Paper Manufacture, volume 7, 85-96.

[13] S.Bussiere, A.Roche and J.Paris. *Analysis and control of white water network perturbations in an integrated newsprint mill.* Pulp and Paper Canada 93:4 1992 41-44.

[14] M. Hagberg and A.Isaksson. *A Paper Machine Benchmark for Control Systems 94.*

[15] P. Tournier. *Analysis of FIA signals using Laguerre network.* 1991.

[16] G.A. Dumont and C.C. Zervos. *Adaptive Control Based On Orthonormal Series Representation.* 2nd IFAC Workshop on Adaptive Systems in Control and Signal Processing 1986 371-376.

[17] C.C.Zervos and G.A.Dumont. *Deterministic adaptive control based on Laguerre series representation.* INT.J. CONTROL, 1988 Vol.48, No. 6, 2333-2359.

[18] C.C. Zervos and G.A.Dumont. *Laguerre functions in stochastic self-tuning control.* 1988 IFAC Workshop on Robust Adaptive Control, Newcastle, 102-107.

[19] C.C. Zervos and G.A.Dumont. *Multivariable self-tuning control based on Laguerre series representation.* Adaptive Control Strategies for Industrial Use, Proceedings of a Workshop, Kananaskis, Canada, 1988 44-57.

[20] G.A.Dumont, C.C.Zervos and G.L.Pageau. *Laguerre-based adaptive control of pH in an industrial bleach plant extraction stage.* Automatica, Vol.26, No.4, pp.781-787, 1990

[21] G.A.Dumont, Y. Fu and A.L. Elshafei. *Orthonormal functions in identification and adaptive control.* ITAC 91 Intelligent Tuning and Adaptive Control, 1991.

[22] A.L. Elshafei, G.A.Dumont and A.Elnaggar. *Adaptive GPC based on Laguerre-filters modelling.* Automatica, Vol.30, No.12, pp. 1913-1920, 1994.

[23] B.Yeager. *The Key to Consistency Lies under the Wire.* Pulp Pap. Int. 38, no.2: 47,49,51, February 1996.

[24] B.Yeager. *Under-the-Wire Scanning Provides Window into Machine Wet End.* Pulp and Paper, 70, no.3: 49-50, 53-54, 57. March 1996.

[25] M.Whitaker. *Optimising Formation Through Consistency Measurement - a Wet-End Revolution.* Pap. Technol. 36, no. 2: 22-26. March 1995.

[26] H. Wang. *Quantitative Adaptive Robust Control Based on a Robust Frequency Domain Estimator.* Ph.D. thesis, Dept. of Electrical Engineering, UBC, 1992

[27] K.J.Astrom and B. Wittenmark. *Adaptive Control.*

[28] Y.Fu and G.A.Dumont. *An Optimum time Scale for Discrete Laguerre Network.* IEEE Transactions on Automatic Control, Vol.38, No.6 pp.934-938, 1993

[29] D.W.Clarke, C.Mohtadi and P.S.Tuffs. *Generalized Predictive Control-Part I. The Basic Algorithm.* Automatica, Vol.23, No. 2, pp 137-148, 1987

[30] K.Y.Kwok and S.L.Shah. *Long-range Predictive Control with a Terminal Matching Condition.* Chemical Engineering Science, Vol. 49, No. 9,pp.1287-1300, 1994

[31] R. Bitmead, M. Gevers and V. Wertz. *Adaptive Optimal Control, The Thinking Man's GPC.* Prentice Hall, Englewood Cliffs, NJ.

[32] R. Soeterboek. *Predictive Control-A Unified Approach.* Prentice Hall

[33] A.L. Elshafei. *Adaptive Predictive Control: Analysis and Expert Implementation.* Ph.D. thesis, Dept. of Electrical Engineering, UBC, 1991

Appendix

Program 1

%%% RLS parameter estimation using Laguerre model %%%

```
%~*~*~*~*~*~*~*~*~*~*~*~*~*~*~*~*~*~*~*~*~*~*~*~*~%

function [sys, x0]=slagu(t,x,u,flag,n, a, forget)

% Parameters
%       n=8;                % the order of Laguerre model (mask)
%       a=0.8;              % Laguerre filter pole (mask)
%       forget=1;           % forgetting factor in the recursive least algorithm (mask)

        b=1+n+n+n*n;        % the number of states

if flag == 0

        % Initial conditions:

%       c=zeros(1,n);       % Laguerre model coefficients
%       l=[zeros(1,n)]';    % Laguerre model states
        p=1000*eye(n);      % error covariance matrix

        sys=[0,b,(n+1),2,0,2];  % size information
        x0=[zeros((n+n+1),1); p(:)];

elseif flag == 2
        % RLS Laguerre coefficient estimation
        z=u';
        c=[x(2:(n+1))]'; l=x((n+2):(n+n+1)); p=reshape(x((n+n+2):b),n,n);
        [c, l, p] = lagu_rls(z,c,l,p,a,forget);
        y=c*l;
        x=[y; c'; l; p(:)];
        sys=x;

elseif flag == 3
        % Output and Laguerre coefficients
        sys=[x(1:(n+1))];
else
        % Otherwise, no need to return anything
        sys=[];
end
```

Program 2

%%% GPC control using Laguerre model %%%

```
%~*~*~*~*~*~*~*~*~*~*~*~*~*~*~*~*~*~*~*~*~*~*~*~*~*~*~*~%
function [sys, x0]=slaguc(t,x,u,flag,n, a, forget)
% Parameters
%     n=12;                 % the order of Laguerre model (mask)
%     a=0.942;              % Laguerre filter pole (mask)
%     forget=1;             % forgetting factor in the recursive least algorithm (mask)

      n1=80; n2=100;              % Minimum and maximum output horizon
%     nu=1;                 % Control horizon
%     beta=0.1;             % control increment weighting
      nn=[80,100,1,0.1];    % GPC tuning parameters
      pyr                   % Program for reference trajectory

c=[1.8951 6.3968 2.4267 -1.1200 1.0462 2.0494 -2.7392 4.9367 -4.2792 3.7254 -2.0496 1.2049];
                            % Laguerre coefficients
      b=1+n+1;              % the number of states

if flag == 0

  % Initial conditions:
      sys=[0,b,2,2,0,2];                % size information
      x0=[zeros((n+2),1)];              % initial states

elseif flag == 2
      z=u';                     % S function inputs

  % GPC control signal
      [U,l]=lagu_gpc(a,c, yr((t+n1):(t+n2))',[z(1) z(2)],x(2:(n+1)),nn);  % GPC control
      y=c*l;

  % Return states
      x=[y; l; U];
      sys=x;

elseif flag == 3
  % Output and control signal
      sys=[x(1);x(b)];
else
  % Otherwise, no need to return anything
      sys=[];
end;
```

Program 3

%%% Adaptive GPC control using Laguerre model %%%

```
%~*~*~*~*~*~*~*~*~*~*~*~*~*~*~*~*~*~*~*~*~*~*~*~*~%
function [sys, x0]=slaguc(t,x,u,flag,n, a, forget)

% Parameters
%      n=12;                % the order of Laguerre model (mask)
%      a=0.942;             % Laguerre filter pole (mask)
%      forget=1;            % forgetting factor in the recursive least algorithm (mask)

       n1=60; n2=100;             % Minimum and maximum output horizon
%      nu=1;                % Control horizon
%      beta=0.1;            % control increment weighting
       nn=[60,100,1,0.1];   % GPC tuning parameters
       pyr                  % Program for reference trajectory
       b=1+n+n+n+n*n+1;           % the number of states
if flag == 0
  % Initial conditions:
       p=1000*eye(n);       % error covariance matrix
       sys=[0,b,2,2,0,2];             % size information
       x0=[zeros((n+n+n+1),1); p(:);0.2368];        % initial states

elseif flag == 2
  % RLS Laguerre coefficient estimation
       z=u';                     % S function inputs
       c=[x(2:(n+1))]'; l=x((n+2):(n+n+1)); p=reshape(x((n+n+n+2):(b-1)),n,n);
       [c, l, p] = lagu_rls(z,c,l,p,a,forget);
       y=c*l;
  % GPC control signal
       [U,dl]=lagu_gpc(a,c,yr((t+n1):(t+n2))',[z(1) z(2)],x((2*n+2):(3*n+1)),nn);  % GPC control

  % Return states
       x=[y; c'; l; dl; p(:); U];
       sys=x;

elseif flag == 3
  % Output and control signal
       sys=[x(1);x(b)];

else
  % Otherwise, no need to return anything
       sys=[];
end;
```